

Example of a **geometrical description** of M-ary QAM:
(QAM – OFDM – MIMO)

“From signal waveforms to signal points”

- The **signal space** concept is general and powerful.
- Increased insight and understanding.
- Improved analysis and implementations.
- We can understand more complicated systems.

$$\boxed{s_\ell(t) = A_\ell g(t) \cos(2\pi f_c t) - B_\ell g(t) \sin(2\pi f_c t)} \quad \ell = 0, 1, \dots, M - 1 \quad (2.87)$$

$$s_\ell(t) = \underbrace{A_\ell \sqrt{E_g/2}}_{s_{\ell,1}} \phi_1(t) + \underbrace{B_\ell \sqrt{E_g/2}}_{s_{\ell,2}} \phi_2(t) \quad (2.99)$$

$$\phi_1(t) = \frac{g(t) \cos(2\pi f_c t)}{\sqrt{E_g/2}} \quad (2.100)$$

$$\phi_2(t) = -\frac{g(t) \sin(2\pi f_c t)}{\sqrt{E_g/2}} \quad (2.101)$$

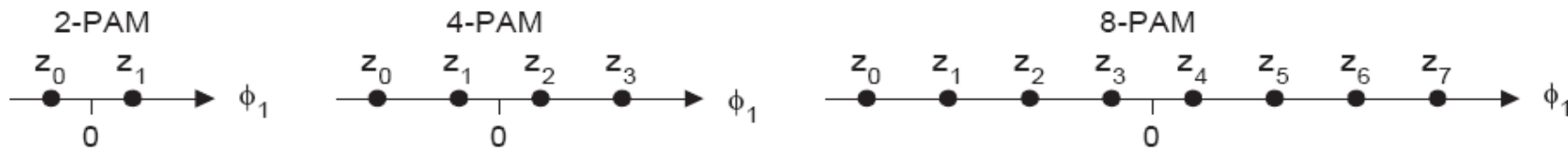
$$z_j(t) = \sum_{\ell=1}^N z_{j,\ell} \phi_{\ell}(t) = z_{j,1} \phi_1(t) + z_{j,2} \phi_2(t) + \dots + z_{j,N} \phi_N(t)$$

(5.1)

$$\int_0^{T_s} \phi_i(t) \phi_j(t) dt = \begin{cases} 1 & , \quad i = j \\ 0 & , \quad i \neq j \end{cases} \quad i, j = 1, 2, \dots, N \quad (5.2)$$

$$z_j(t) \iff z_j = (z_{j,1}, z_{j,2}, \dots, z_{j,N})^{tr}, \quad j = 0, 1, \dots, M-1 \quad (5.3)$$

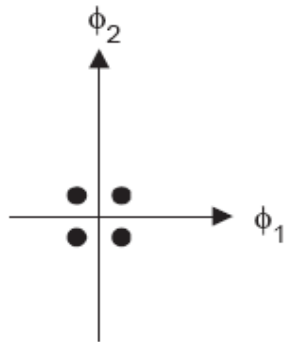
$$s_{\ell}(t) = A_{\ell} g(t) = A_{\ell} \sqrt{E_g} \cdot \underbrace{\frac{g(t)}{\sqrt{E_g}}}_{\phi_1(t)} = \underbrace{A_{\ell} \sqrt{E_g}}_{s_{\ell,1}} \cdot \phi_1(t) = s_{\ell,1} \cdot \phi_1(t) \quad (2.51)$$



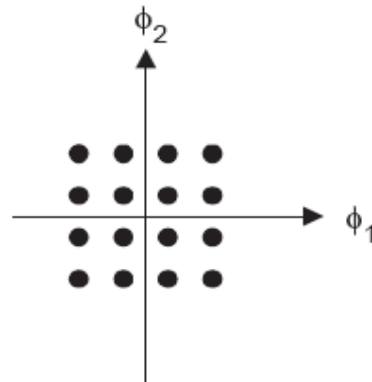
As examples, let us collect some results from subsection 2.4:

$$\begin{aligned}
 \text{M-ary PAM:} \quad & z_j = ((-M + 1 + 2j)\sqrt{E_g}), & N = 1 \\
 \text{M-ary PSK:} \quad & z_j = \left(\cos(\nu_j)\sqrt{\frac{E_g}{2}}, \sin(\nu_j)\sqrt{\frac{E_g}{2}} \right)^{tr}, & N = 2 \\
 \text{M-ary FSK:} \quad & z_j = (0, 0, \dots, \sqrt{E_j}, 0, 0, 0)^{tr}, & N = M \\
 \text{M-ary QAM:} \quad & z_j = \left(A_j\sqrt{\frac{E_g}{2}}, B_j\sqrt{\frac{E_g}{2}} \right)^{tr}, & N = 2
 \end{aligned} \tag{5.4}$$

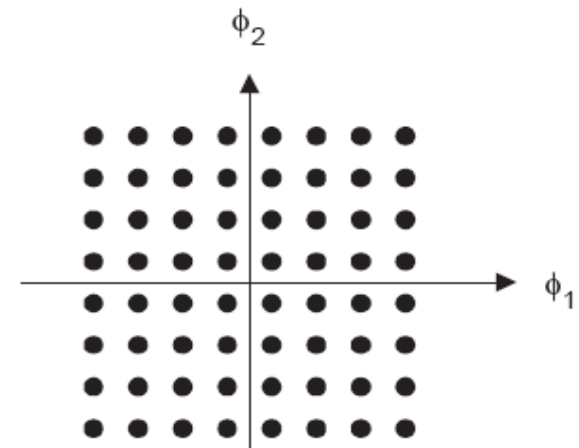
4-QAM



16-QAM



64-QAM



$$\begin{aligned}
 E_j &= \int_0^{T_s} z_j^2(t) dt = \sum_{\ell=1}^N z_{j,\ell}^2 = z_j^{tr} z_j \\
 D_{i,j}^2 &= \int_0^{T_s} (z_i(t) - z_j(t))^2 dt = \sum_{\ell=1}^N (z_{i,\ell} - z_{j,\ell})^2 = \quad , \quad i,j=0,1,\dots,M-1 \\
 &= E_i + E_j - 2z_i^{tr} z_j
 \end{aligned}$$

(5.8)

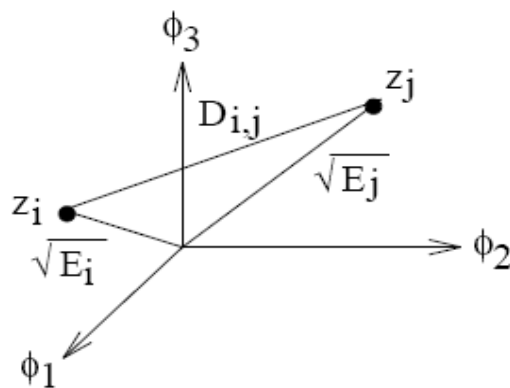
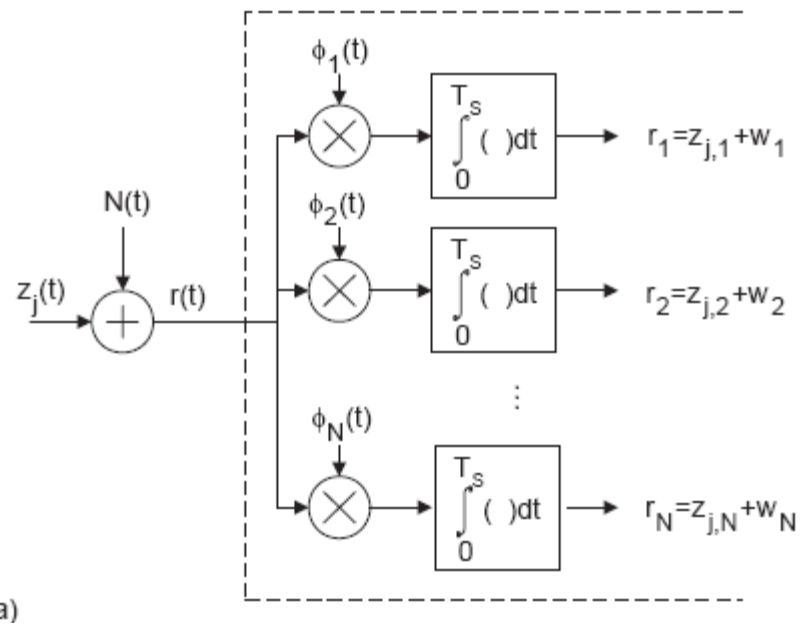


Figure 5.3: Illustrating E_ℓ and $D_{i,j}$ in signal space.



a)

Figure 5.6: a) The first step in the MAP receiver;

$$\int_0^{T_s} z_j(t) \phi_\ell(t) dt = \int_0^{T_s} \sum_{n=1}^N z_{j,n} \phi_n(t) \phi_\ell(t) dt = \sum_{n=1}^N z_{j,n} \int_0^{T_s} \phi_n(t) \phi_\ell(t) dt = z_{j,\ell} \quad (5.12)$$

After the correlators we obtain a **received noisy signalpoint** r !

$$\boxed{\begin{aligned} E\{w_\ell\} &= 0 \\ \sigma_\ell^2 &= E\{w_\ell^2\} = N_0/2 \\ E\{w_\ell w_m\} &= 0, \quad \ell \neq m \end{aligned}} \quad \ell = 1, 2, \dots, N \quad (5.22)$$

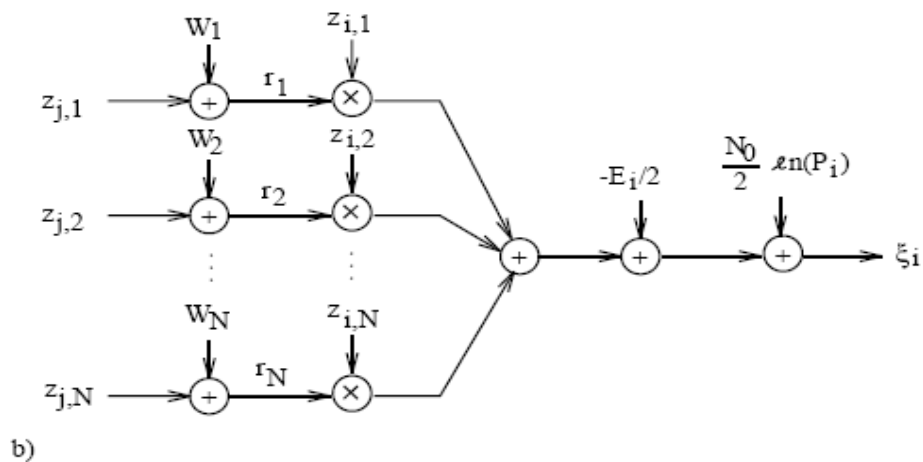
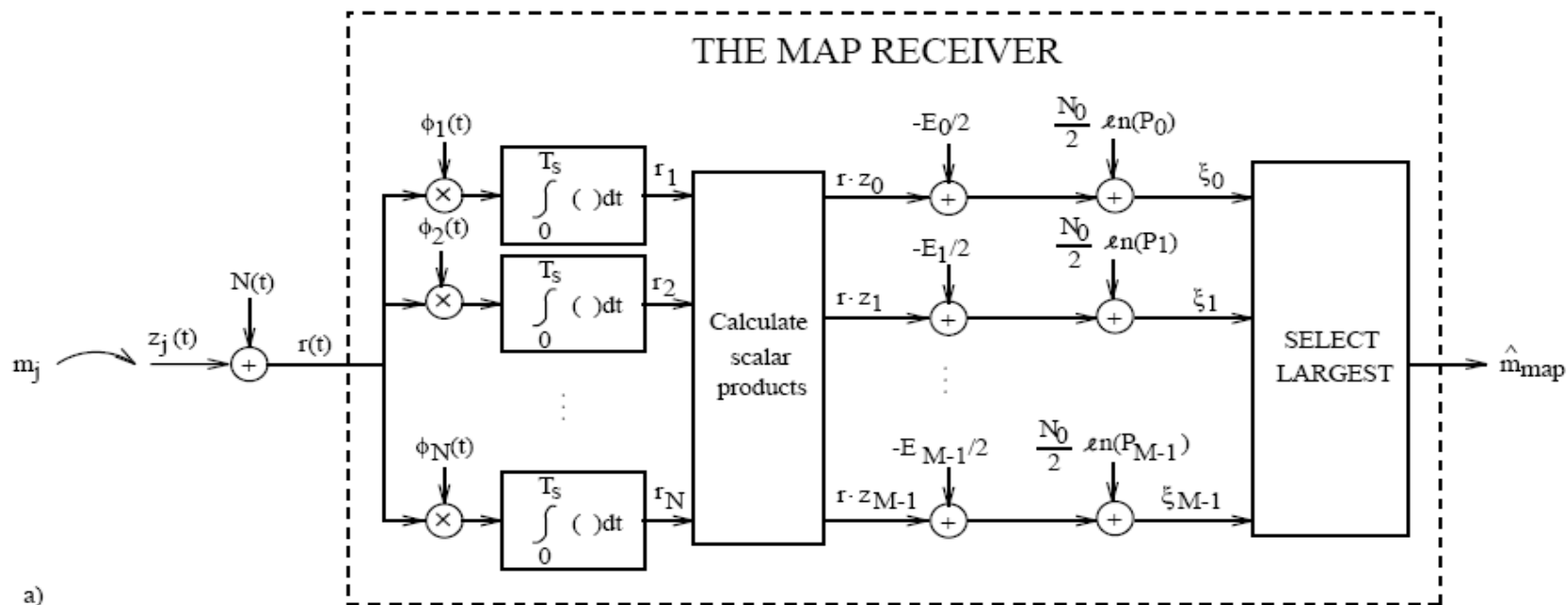


Figure 5.8: a) The MAP receiver; b) A discrete-time model of the decision variable ξ_i .

$$\boxed{\mathbf{r} = \mathbf{z}_j + \mathbf{w}} \quad (5.18)$$

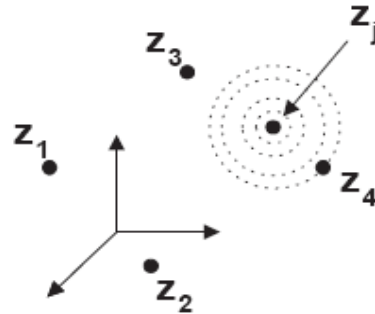


Figure 5.7: Illustrating “the cloud” of noise in \mathbf{r} if message m_j is sent.

The distance between the received noisy signal point \mathbf{r} and the signal point \mathbf{z}_j is:

$$\boxed{D_{r,j}^2 = (\mathbf{r} - \mathbf{z}_j)^{tr} (\mathbf{r} - \mathbf{z}_j) = \sum_{\ell=1}^N (r_\ell - z_{j,\ell})^2} \quad (5.24)$$

MAP decision rule:

$$\hat{m}(\mathbf{r}) = m_\ell \Leftrightarrow \min_{\{i\}} \{D_{r,i}^2 - N_0 \ln(P_i)\} = D_{r,\ell}^2 - N_0 \ln(P_\ell) \quad (5.25)$$
$$\Downarrow$$
$$\max_{\{i\}} \{\mathbf{r}^{tr} \mathbf{z}_i + c_i\} = \mathbf{r}^{tr} \mathbf{z}_\ell + c_\ell$$

ML decision rule = minimum distance decision rule:

In the MAP decision rule (5.25)–(5.26) we observe that if $P_i = 1/M$, then the terms $N_0 \ln(P_\ell)$ can be ignored, resulting in the decision rule

$$\hat{m}(r) = m_\ell \Leftrightarrow \min_{\{i\}} D_{r,i}^2 = D_{r,\ell}^2 \quad (5.28)$$

Hence, *if $P_i = 1/M$, then the ML decision rule is obtained as the minimum Euclidean distance decision rule.* Observe also in (5.25) that

5.1.3 The Symbol Error Probability for M-ary PAM

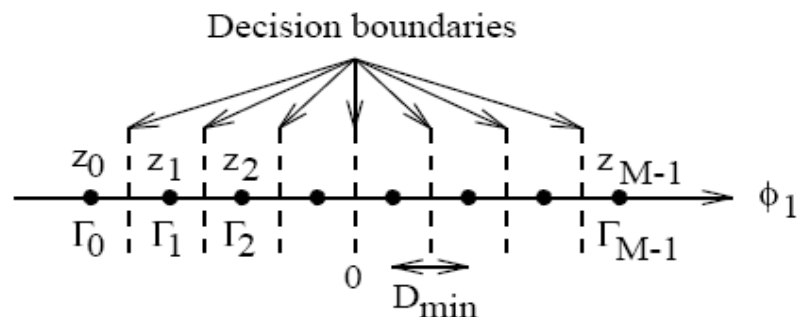


Figure 5.9: The signal space for M-ary PAM with equispaced amplitudes, centered symmetrically around zero (see (5.4)).

$$\begin{aligned} \text{Prob}\{\text{error}|m_0 \text{ sent}\} &= \text{Prob}\left\{w_1 > \frac{D_{\min}}{2}\right\} = \\ &= \text{Prob}\left\{\frac{w_1}{\sqrt{N_0/2}} > \frac{D_{\min}}{\sqrt{2N_0}}\right\} = Q\left(\sqrt{\frac{D_{\min}^2}{2N_0}}\right) \end{aligned} \quad (5.31)$$

$$\begin{aligned}
\text{Prob}\{\text{error}|m_1 \text{ sent}\} &= \text{Prob}\left\{w_1 < -\frac{D_{\min}}{2} \text{ or } w_1 > \frac{D_{\min}}{2}\right\} = \\
&= \text{Prob}\left\{\frac{w_1}{\sqrt{N_0/2}} < -\frac{D_{\min}}{\sqrt{2N_0}}\right\} + \text{Prob}\left\{\frac{w_1}{\sqrt{N_0/2}} > \frac{D_{\min}}{\sqrt{2N_0}}\right\} = \\
&= 2Q\left(\sqrt{\frac{D_{\min}^2}{2N_0}}\right)
\end{aligned} \tag{5.32}$$

$$P_s = \sum_{j=0}^{M-1} P_j \text{Prob}\{\text{error}|m_j \text{ sent}\}$$

$$\boxed{P_s = \frac{2}{M} (M-1)Q\left(\sqrt{\frac{D_{\min}^2}{2N_0}}\right)}, \quad \text{M-ary PAM} \tag{5.35}$$

P_s is shown in Figure 5.13 on page 362.

5.1.4 The Symbol Error Probability for QPSK

$$r(t) = z_j(t) + N(t), \quad 0 \leq t \leq T_s, \quad j = 0, 1, \dots, M - 1 \quad (5.13)$$

$$r_1 = z_{j,1} + w_1 \quad (5.36)$$

$$r_2 = z_{j,2} + w_2 \quad (5.37)$$

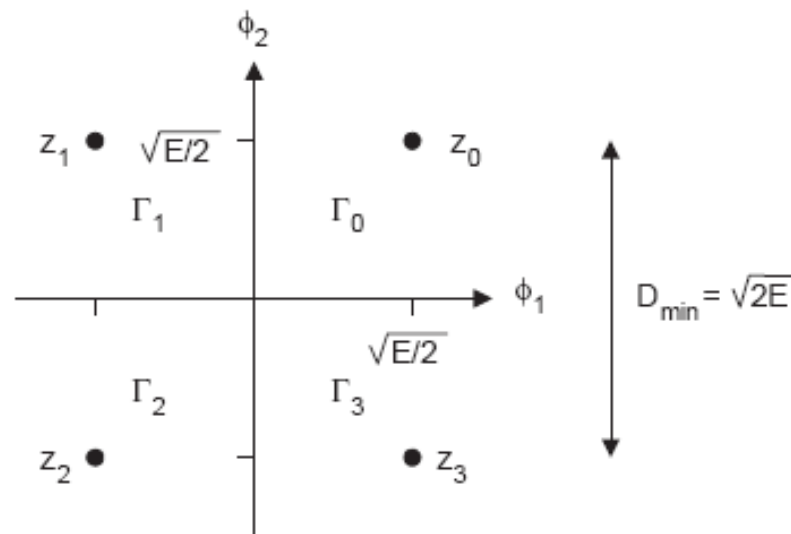


Figure 5.10: The signal space for QPSK if $\nu_\ell = (2\pi \frac{\ell}{M} + \pi/4)$ (see (5.4)).

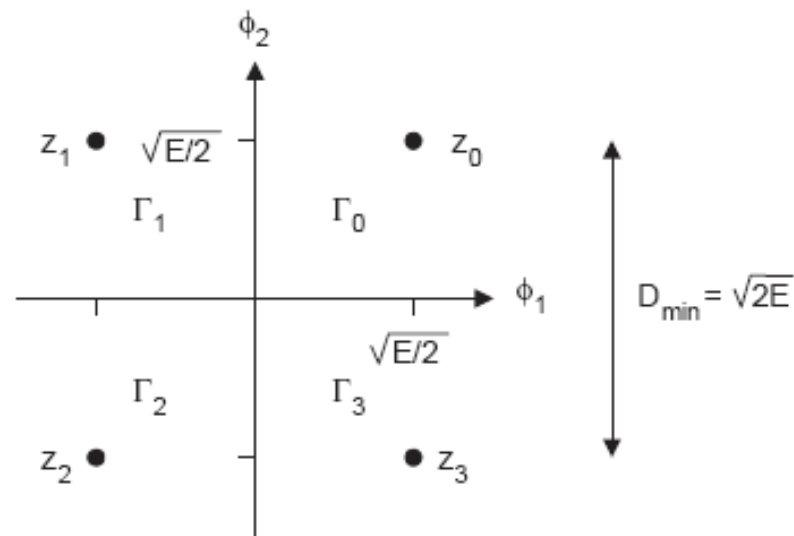


Figure 5.10: The signal space for QPSK if $\nu_\ell = (2\pi \frac{\ell}{M} + \pi/4)$ (see (5.4)).

$$\begin{aligned}
 & Prob\{\text{error}|m_0 \text{ sent}\} = 1 - Prob\{\text{correct decision}|m_0 \text{ sent}\} = \\
 & = 1 - Prob\left\{w_1 \geq -\frac{D_{\min}}{2}, w_2 \geq -\frac{D_{\min}}{2}\right\} = \\
 & = 1 - Prob\left\{w_1 \geq -\frac{D_{\min}}{2}\right\} Prob\left\{w_2 \geq -\frac{D_{\min}}{2}\right\} = \\
 & = 1 - \left[1 - Q\left(\sqrt{\frac{D_{\min}^2}{2N_0}}\right)\right]^2 = 2Q\left(\sqrt{\frac{D_{\min}^2}{2N_0}}\right) - Q^2\left(\sqrt{\frac{D_{\min}^2}{2N_0}}\right) \stackrel{\text{symmetry}}{\downarrow} = \\
 & = Prob\{\text{error}|m_j \text{ sent}\}, j = 0, 1, 2, 3 \tag{5.38}
 \end{aligned}$$

5.1.5 The Symbol Error Probability for M-ary PSK

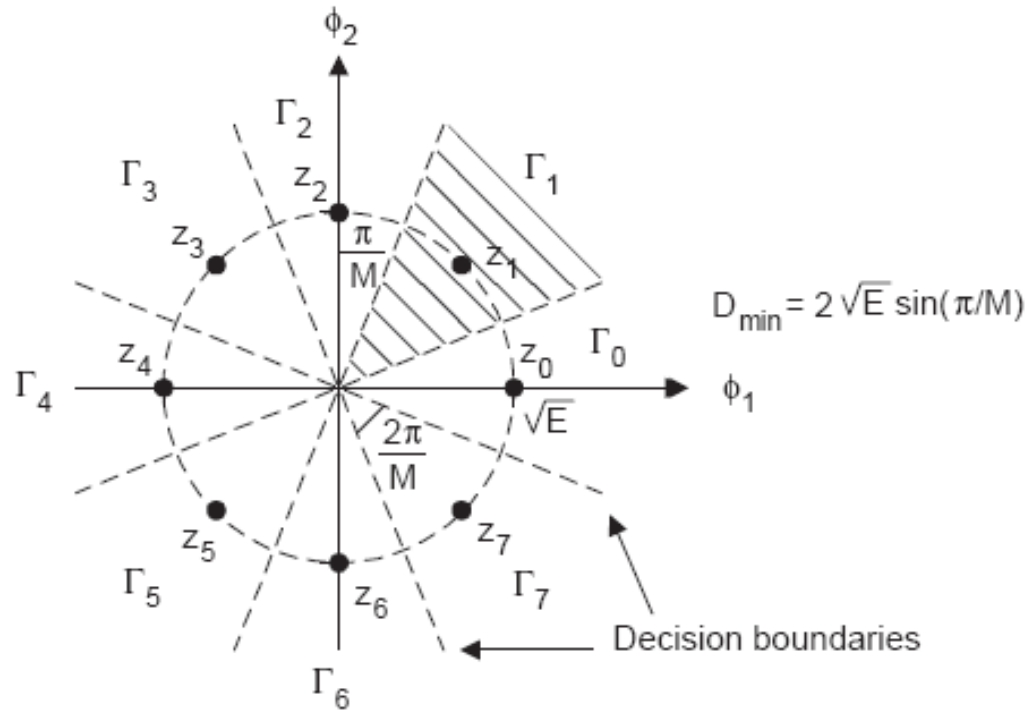


Figure 5.11: The signal space for M-ary PSK if $\nu_\ell = 2\pi\ell/M$ (see (5.4)). $M = 8$ in this figure.

$$\boxed{
 \begin{aligned}
 Q\left(\sqrt{\frac{D_{\min}^2}{2N_0}}\right) &\leq P_s < 2Q\left(\sqrt{\frac{D_{\min}^2}{2N_0}}\right), \text{ M-ary PSK} \\
 D_{\min}^2 &= 4E \sin^2(\pi/M)
 \end{aligned}
 } \quad (5.43)$$

5.1.6 The Symbol Error Probability for M-ary QAM

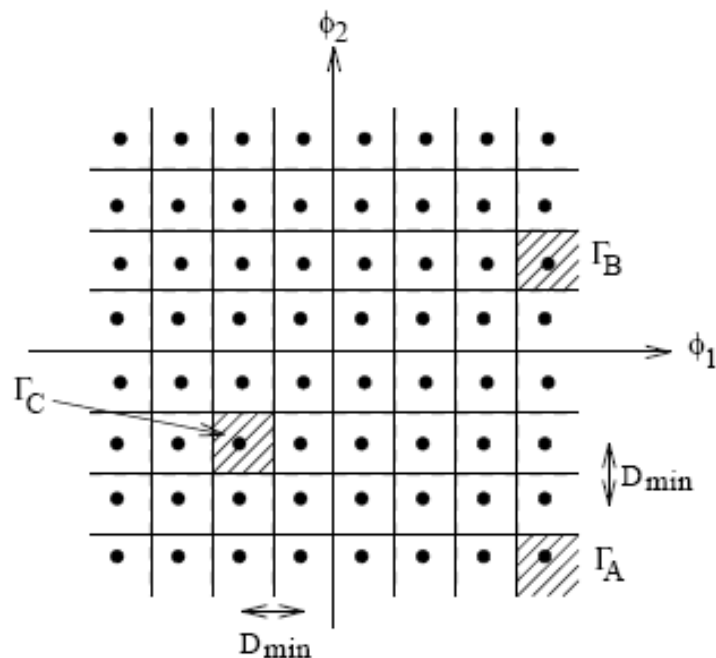


Figure 5.12: The signal space for M-ary QAM (compare with (5.4), see also Subsection 2.4.5.1). $M=64$ in this figure.

Γ_A : Compare with (5.39).

$$Prob\{\text{error}|m_A \text{ sent}\} = 2Q \left(\sqrt{\frac{D_{\min}^2}{2N_0}} \right) - Q^2 \left(\sqrt{\frac{D_{\min}^2}{2N_0}} \right) \quad (5.46)$$

Γ_B :

$$\begin{aligned} Prob\{\text{error}|m_B \text{ sent}\} &= \\ &= 1 - Prob \left\{ w_1 > -\frac{D_{\min}}{2}, -\frac{D_{\min}}{2} \leq w_2 \leq \frac{D_{\min}}{2} \right\} = \\ &= 1 - \left(1 - Q \left(\sqrt{\frac{D_{\min}^2}{2N_0}} \right) \right) \left(1 - 2Q \left(\sqrt{\frac{D_{\min}^2}{2N_0}} \right) \right) = \\ &= 3Q \left(\sqrt{\frac{D_{\min}^2}{2N_0}} \right) - 2Q^2 \left(\sqrt{\frac{D_{\min}^2}{2N_0}} \right) \end{aligned} \quad (5.47)$$

Γ_C :

$$\begin{aligned} Prob\{\text{error}|m_C \text{ sent}\} &= \\ &= 1 - Prob \left\{ -\frac{D_{\min}}{2} \leq w_1 \leq \frac{D_{\min}}{2}, -\frac{D_{\min}}{2} \leq w_2 \leq \frac{D_{\min}}{2} \right\} = \\ &= 1 - \left(1 - 2Q \left(\sqrt{\frac{D_{\min}^2}{2N_0}} \right) \right)^2 = \\ &= 4Q \left(\sqrt{\frac{D_{\min}^2}{2N_0}} \right) - 4Q^2 \left(\sqrt{\frac{D_{\min}^2}{2N_0}} \right) \end{aligned} \quad (5.48)$$

$$P_s = \frac{4}{\sqrt{M}} (\sqrt{M}-1) Q \left(\sqrt{\frac{D_{\min}^2}{2N_0}} \right) - \frac{4}{M} (\sqrt{M}-1)^2 Q^2 \left(\sqrt{\frac{D_{\min}^2}{2N_0}} \right), \text{ M-ary QAM} \quad (5.50)$$

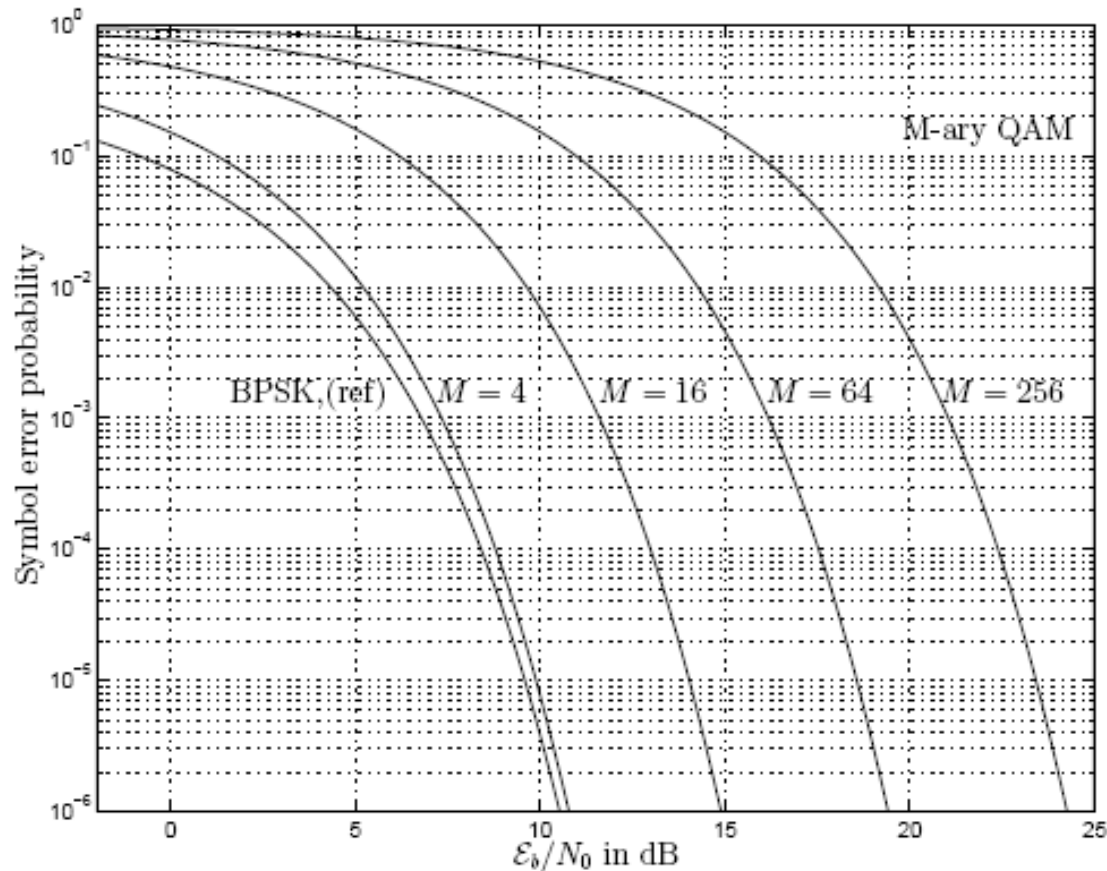


Figure 5.15: The symbol error probability for M-ary QAM, $M = 4, 16, 64, 256$, see Table 5.1. The specific assumptions are given in Subsection 2.4.5.1 and in Subsection 5.1.6. The bit error probability for BPSK is also given as a reference ($= Q(\sqrt{2\mathcal{E}_b/N_0})$).

5.2.2 Power and Bandwidth Efficiency

We saw in (5.60) that the information bit rate R_b is limited by d_{\min}^2 , c , P_z , N_0 and $P_{s,req}$. Let us divide both sides in (5.60) with the bandwidth W ,

$$\rho \leq \frac{d_{\min}^2}{\mathcal{X}} \cdot \frac{P_z}{N_0 W} = \frac{d_{\min}^2}{\mathcal{X}} \cdot \mathcal{SNR}_r \quad (5.61)$$

Note that the bandwidth efficiency ρ is limited by d_{\min}^2 , c , $P_{s,req}$, and by the **received signal-to-noise power ratio** $\mathcal{SNR}_r = P_z/N_0 W$ within the signal bandwidth W . The bandwidth W is the physical bandwidth defined on the

5.2.3 Shannon's Capacity Theorem

In Shannons capacity theorem, [54], [68], [20], [43], for the bandlimited flat ($|H(f)|^2 = \alpha^2$ within the bandwidth W) AWGN channel, the capacity \mathcal{C} for this channel is (in bits per second),

$$\mathcal{C} = W \log_2 \left(1 + \frac{P_z}{N_0 W} \right), [b/s] \quad (5.62)$$

where W is the physical bandwidth measured on the positive frequency axis containing **all** the signal power. This remarkable theorem states that ([43], [68]): **There exists** at least one signal construction method that achieves an arbitrary small error probability, if the bit rate $R_b < \mathcal{C}$. If $R_b > \mathcal{C}$, then the error probability P_s is high for every possible signal construction method.

$$\mathcal{C} = W \log_2 \left(1 + \frac{\mathcal{P}_z}{N_0 W} \right), \text{ [b/s]} \quad (5.62)$$

$$\lim_{W \rightarrow \infty} \mathcal{C} = \lim_{W \rightarrow \infty} \frac{W}{\ln(2)} \ln \left(1 + \frac{\mathcal{P}_z}{N_0 W} \right) = \frac{\mathcal{P}_z}{N_0 \ln(2)} \quad (5.63)$$

$$\frac{\mathcal{C}}{W} = \log_2 \left(1 + \frac{\mathcal{P}_z}{N_0 W} \right) = \log_2 \left(1 + \frac{\mathcal{C}}{W} \cdot \frac{\mathcal{E}_b}{N_0} \right), \text{ [bps/Hz]}$$

or equivalently,

$$\frac{\mathcal{E}_b}{N_0} = \frac{2^{\mathcal{C}/W} - 1}{\mathcal{C}/W} \quad (5.64)$$

Since \mathcal{C} is the maximum bit rate, \mathcal{E}_b here represents the minimum average received energy per information bit, for a given \mathcal{P}_z , $\mathcal{P}_z = \mathcal{C}\mathcal{E}_b$.

$$\frac{\mathcal{P}_z}{N_0 W} = \frac{\mathcal{C}}{W} \cdot \frac{\mathcal{E}_b}{N_0} = 2^{\mathcal{C}/W} - 1 \quad (5.65)$$

5.2.3.1 Shannon Capacity for General $|H(f)|^2$ and $R_N(f)$

1. For a given average transmitted signal power P_{sent} , and channel quality function $q_{ch}(f) = |H(f)|^2/R_N(f)$, the parameter B below should first be determined,

$$P_{sent} = \int_{\Omega} \left(B - \frac{R_N(f)}{|H(f)|^2} \right) df \quad (5.68)$$

This is referred to as "**waterfilling**"!

2. The capacity C is then found as,

$$C = \int_{\Omega} \frac{1}{2} \log_2 \left(\frac{|H(f)|^2}{R_N(f)} \cdot B \right) df \quad (5.70)$$

5.4.1 Diversity: Introductory Concepts

“Dont put all eggs in the same basket”

Assume that each message is sent in N dimensions (time/frequency/space etc)

$$s_j(t) = \sum_{n=1}^N s_{j,n} \phi_n(t) , \quad j = 0, 1, \dots, M - 1 \quad (5.79)$$

Assume independent attenuations in each dimension:

$$r(t) = z_j(t) + N(t) = \sum_{n=1}^N \alpha_n s_{j,n} \phi_n(t) + N(t) \quad (5.80)$$

$$z_j = \begin{pmatrix} \alpha_1 & & & \mathbf{0} \\ & \alpha_2 & & \\ & & \ddots & \\ \mathbf{0} & & & \alpha_N \end{pmatrix} \begin{pmatrix} s_{j,1} \\ \vdots \\ s_{j,N} \end{pmatrix} = \begin{pmatrix} \alpha_1 s_{j,1} \\ \vdots \\ \alpha_N s_{j,N} \end{pmatrix} \quad (5.81)$$

Note: It can be very “dangerous” to use only one (i.e. N=1) dimension!

We now introduce the concept of **diversity** in connection with Figure 5.21 and (5.80). Diversity is often used, e.g., for so-called **fading** channels (randomly varying signal levels, see Chapter 9), to improve the error probability. *Diversity can be obtained by spreading the same message over many dimensions.* Hence, in the receiver, message m_j has coordinates in, say L , dimensions. Let p denote the probability that a received signal is seriously distorted in any single dimension. The basic idea with diversity is that the probability for large distortions in **all** dimensions ($\approx p^L$) is significantly lower than p . Observe that this requires that the distortions in each dimension are essentially independent. So, intuitively speaking, there is a high probability that a few message carrying coordinates “survive” the channel without too much damage, and it is these coordinates that the receiver bases its decision on. Compare with Figure 5.21b,c assuming some of the α_n ’s are close to zero. It should also be mentioned here that there is a close relationship between the concept of diversity and the concept of **coding**.

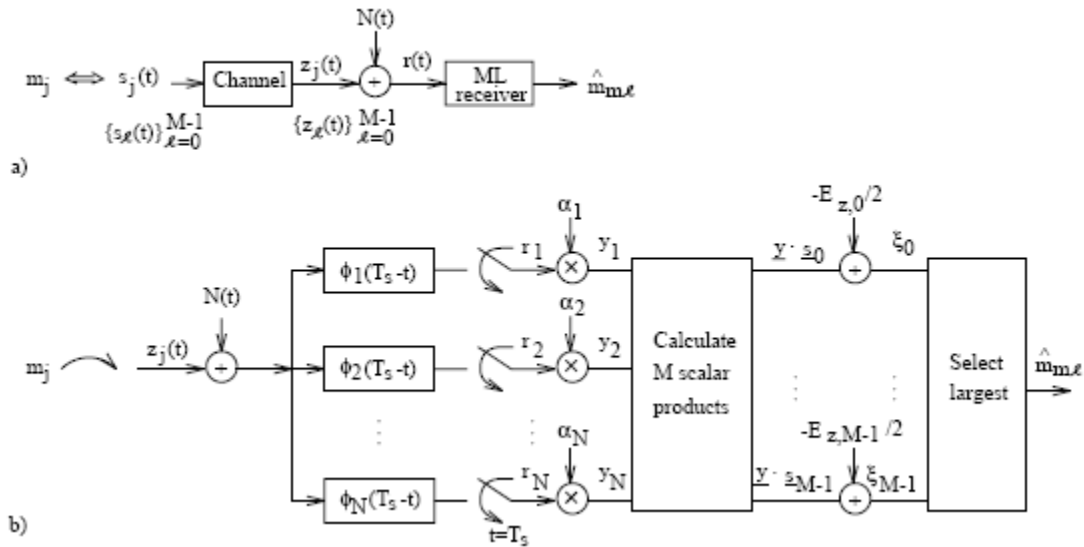


Figure 5.21:

a) The digital communication system; b) The ML receiver, assuming (5.80);

Observe that the channel attenuations are used as *multipliers in the receiver* according to the receiver structure in figure 5.8a on page 341!

EXAMPLE 5.23

Assume a binary communication system with equiprobable antipodal signal alternatives,

$$s_1(t) = -s_0(t) = \sum_{k=1}^K g_k(t), \quad 0 \leq t \leq T_b$$

Let $E_{b, \text{sent}}$ denote the average transmitted energy per information bit, i.e. $E_{s_1} = E_{s_0} = E_{b, \text{sent}}$. It is also assumed that the individual pulses $g_k(t)$ are such that

$$\int_0^{T_b} g_i(t)g_j(t) dt = \begin{cases} E_{b, \text{sent}}/K & , \quad i = j \\ 0 & , \quad i \neq j \end{cases}$$

We can therefore define (sent) basis functions as,

$$\phi_k(t) = \frac{g_k(t)}{\sqrt{E_{b, \text{sent}}/K}}, \quad k = 1, 2, \dots, K$$

and the signal energy $E_{b, \text{sent}}/K$ is sent in each of the K dimensions.

Observe that the situation studied in this example applies to several kinds of diversity, e.g., time- and/or frequency-diversity, depending on how the pulses $g_k(t)$ are chosen.

The communication channel is assumed to be such that the received signal alternatives are,

$$z_1(t) = -z_0(t) = \sum_{k=1}^K \alpha_k g_k(t) = \sum_{k=1}^K \underbrace{\alpha_k \sqrt{\frac{E_{b, \text{sent}}}{K}}}_{z_{1,k}} \phi_k(t)$$

and they are disturbed by AWGN $N(t)$ with power spectral density $R_N(f) = N_0/2$. Note that the channel coefficients $\{\alpha_k\}_{k=1}^K$ multiply the signal in each dimension, respectively. The ideal ML receiver is used and it is assumed that perfect estimates of the channel coefficients are available to the receiver.

- a) Assume that the channel parameters $\{\alpha_k\}_{k=1}^K$ are known to the receiver. Determine an expression of P_b that includes $E_{b, \text{sent}}$.
- b) Suggest a receiver structure for the case in a).

Solution:

a)

$$P_b = Q\left(\sqrt{2E_b/N_0}\right)$$

$$\varepsilon_b = \frac{E_{z_0} + E_{z_1}}{2} = E_{z_0} = E_{z_1} = \sum_{k=1}^K z_{j,k}^2 = \frac{E_{b, \text{sent}}}{K} \sum_{k=1}^K \alpha_k^2$$

Hence, we obtain that

$$P_b = Q\left(\sqrt{\frac{2E_{b, \text{sent}}}{N_0 K} \sum_{k=1}^K \alpha_k^2}\right)$$

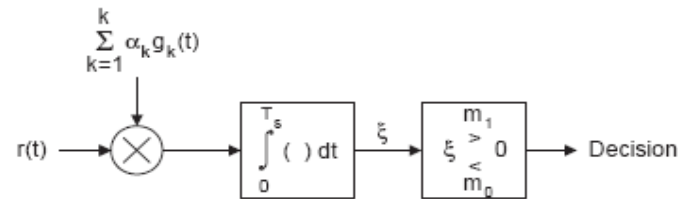
Note that here a K -fold diversity is obtained, in the sense that signal energy from all K dimensions (or “sub-channels”) is efficiently collected and used in the decision process.

Note also that

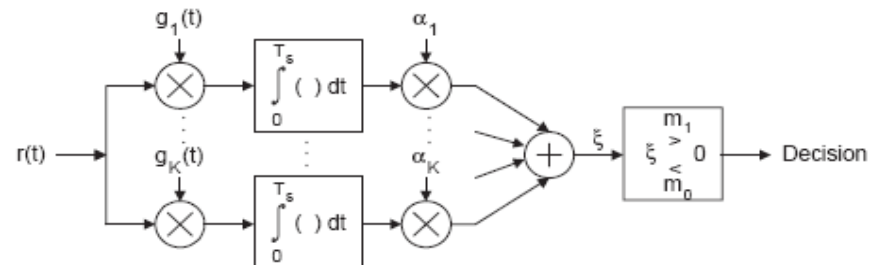
$$D_{s_1, s_0}^2 = 4E_{b, \text{sent}}$$

$$D_{z_1, z_0}^2 = 4E_z = \frac{4E_{b, \text{sent}}}{K} \sum_{k=1}^K \alpha_k^2 = \frac{D_{s_1, s_0}^2}{K} \sum_{k=1}^K \alpha_k^2$$

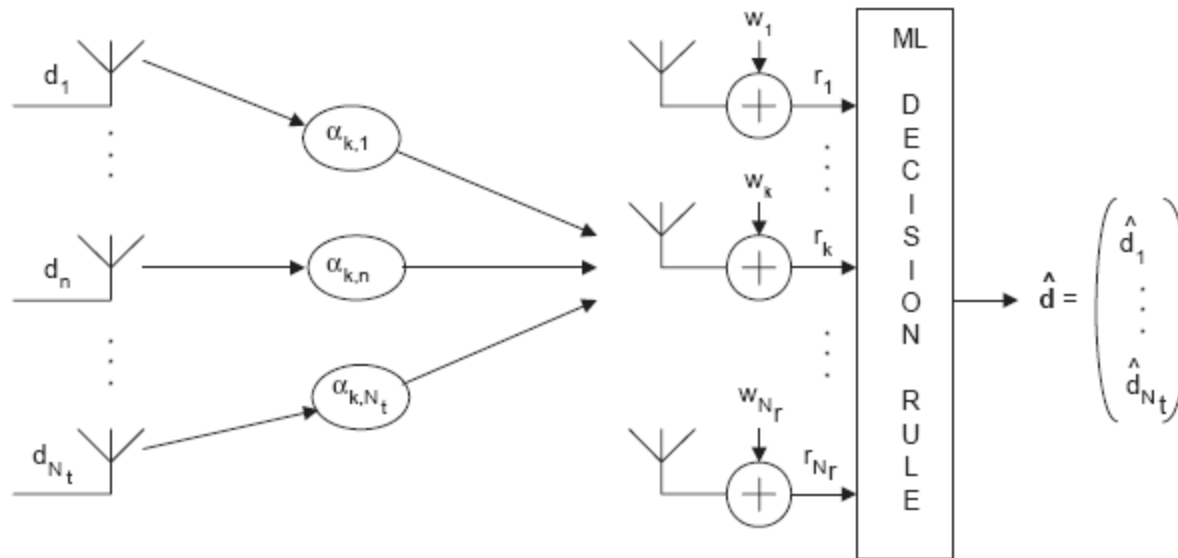
b) From Figure 4.10 on page 247 we obtain the receiver structure below (the constant 2 is ignored in the correlation below),



An equivalent receiver structure is also shown below,



MIMO MODEL



$$r_k = \sum_{n=1}^{N_t} \alpha_{k,n} d_n + w_k$$

$$\mathbf{r} = \begin{pmatrix} r_1 \\ \vdots \\ r_{N_r} \end{pmatrix} = \mathbf{A} \begin{pmatrix} d_1 \\ \vdots \\ d_{N_t} \end{pmatrix} + \begin{pmatrix} w_1 \\ \vdots \\ w_{N_r} \end{pmatrix} = \mathbf{A} \mathbf{d} + \mathbf{w}$$

Assume, e.g., that: $N_t=1$ and data symbol d_1 is binary: $+A$ or $-A$

5.4.1.1 An Example Illustrating Diversity Gains

Here we study the case when the channel parameters $\{\alpha_k\}_{k=1}^K$ have the following properties:

- They are assumed to be independent random variables, and only two values are possible for each α_k .
- Each α_k takes the value α_G (“Good”) with probability P_G , and the value α_B (“Bad”) with probability $P_B = 1 - P_G$.

$$\begin{aligned}\mathcal{E}_b &= E \left\{ \frac{E_{b, \text{sent}}}{K} \sum_{k=1}^K \alpha_k^2 \right\} = E_{b, \text{sent}} E \{ \alpha_k^2 \} = \\ &= E_{b, \text{sent}} (\alpha_G^2 P_G + \alpha_B^2 (1 - P_G))\end{aligned}\tag{5.84}$$

$$\begin{aligned}P_b &= E \left\{ P_{b|\{\alpha_k\}_{k=1}^K} \right\} = E \left\{ Q \left(\sqrt{\frac{2E_{b, \text{sent}}}{N_0 K} \sum_{k=1}^K \alpha_k^2} \right) \right\} = \\ &= E \left\{ Q \left(\sqrt{\frac{2}{\alpha_G^2 P_G + \alpha_B^2 (1 - P_G)} \cdot \frac{\mathcal{E}_b}{N_0} \cdot \frac{1}{K} \sum_{k=1}^K \alpha_k^2} \right) \right\}\end{aligned}\tag{5.85}$$

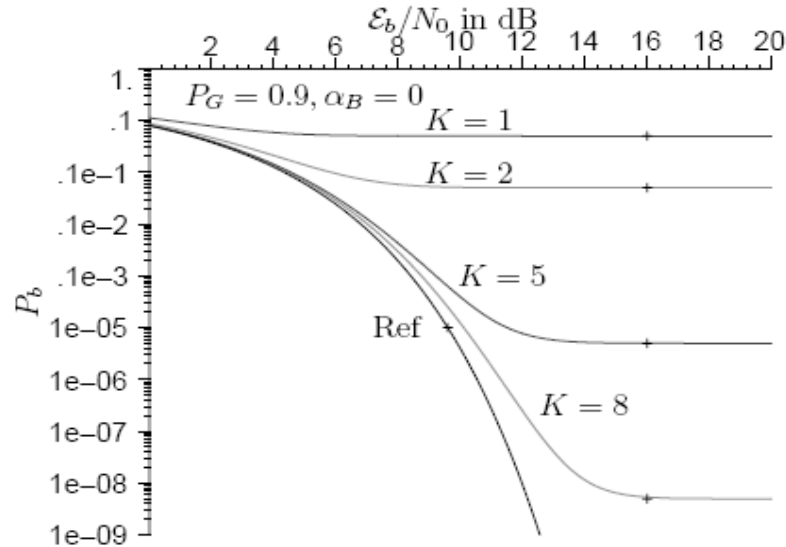


Figure 5.22: The bit error probability versus \mathcal{E}_b/N_0 for the case $P_G = 0.9$ and $\alpha_B = 0$, with $K = 1, 2, 5, 8$.

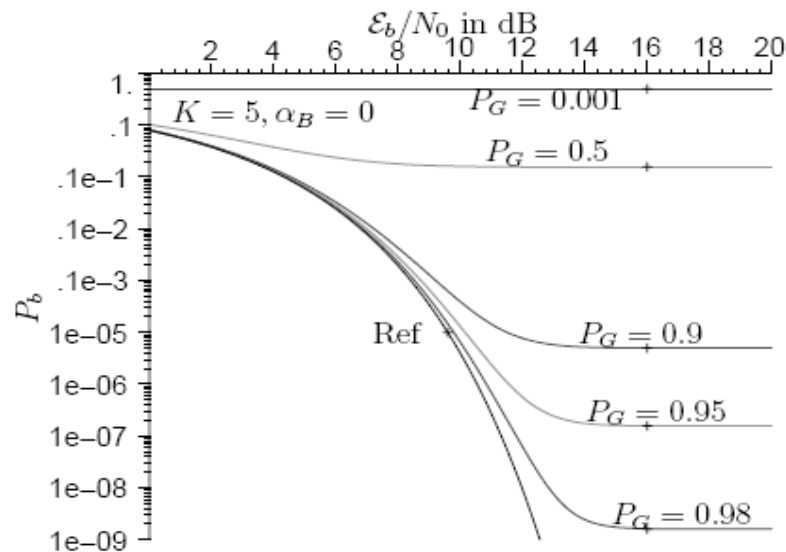


Figure 5.23: The bit error probability versus \mathcal{E}_b/N_0 for the case $K = 5$ and $\alpha_B = 0$, with $P_G = 0.001, 0.5, 0.9, 0.95, 0.98$.

3.4.1 Low-Rate QAM-Type of Input Signals

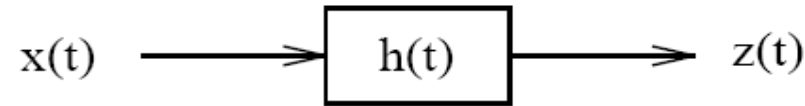


Figure 3.11: Bandpass filtering.

$$x(t) = x_I(t) \cos(\omega_c t) - x_Q(t) \sin(\omega_c t) = \text{Re}\{\tilde{x}(t)e^{j\omega_c t}\} \quad (3.103)$$

$$\tilde{x}(t) = x_I(t) + jx_Q(t) \quad (3.104)$$

This complex signal contains the information!

$$x(t) = x_I(t) \cos(\omega_c t) - x_Q(t) \sin(\omega_c t) = \text{Re}\{\tilde{x}(t)e^{j\omega_c t}\} \quad (3.103)$$

$$\begin{aligned} z(t) &= \int_{-\infty}^{\infty} h(\tau)x(t - \tau)d\tau = \int_{-\infty}^{\infty} h(\tau)\text{Re}\{\tilde{x}(t - \tau)e^{j\omega_c(t-\tau)}\}d\tau = \\ &= \text{Re}\left\{e^{j\omega_c t} \int_{-\infty}^{\infty} h(\tau)\tilde{x}(t - \tau)e^{-j\omega_c\tau} d\tau\right\} \end{aligned} \quad (3.105)$$

3 assumptions:

- 1) The duration of the impulse response $h(t)$ can be considered to be equal to T_h . This means that essentially all the energy in $h(t)$ is assumed to be contained within the time interval $0 \leq t \leq T_h$.
- 2) The input signal is assumed to be a QAM-type of signal with duration $T = T_s$:

$$x(t) = \begin{cases} 0 & , t < 0 \\ A \cos(\omega_c t) - B \sin(\omega_c t) = \sqrt{A^2 + B^2} \cos(\omega_c t + \nu) & , 0 \leq t \leq T_s \\ 0 & , t > T_s \end{cases} \quad (3.106)$$

- 3) $T_s > T_h$ ("low" signaling rate).

$$\tilde{x}(t) = \begin{cases} A + jB = \sqrt{A^2 + B^2} e^{j\nu} & , \quad 0 \leq t \leq T_s \\ 0 & , \quad \text{otherwise} \end{cases} \quad (3.108)$$

$T_h \leq t \leq T_s$:

$$\begin{aligned} z(t) &= \text{Re} \left\{ e^{j\omega_c t} \int_0^{T_h} h(\tau) \sqrt{A^2 + B^2} e^{j\nu} e^{-j\omega_c \tau} d\tau \right\} = \\ &= \text{Re} \{ \sqrt{A^2 + B^2} e^{j\nu} \cdot H(f_c) e^{j\omega_c t} \} = \\ &= |H(f_c)| \sqrt{A^2 + B^2} \cos(\omega_c t + \nu + \phi(f_c)) = A_z \cos(\omega_c t) - B_z \sin(\omega_c t) \end{aligned} \quad (3.109)$$

Hence, a QAM-signal at the output in this time interval!

However, **attenuation and rotation** compared with the input!
Compare with the input $x(t)$ in (3.106)!

$$\begin{aligned} A_z + jB_z &= (A + jB)H(f_c) = \sqrt{A^2 + B^2} |H(f_c)| e^{j(\nu + \phi(f_c))} = \\ &= (A + jB)(H_{Re}(f_c) + jH_{Im}(f_c)) \end{aligned} \quad (3.110)$$

$$\begin{aligned}
 A_z + jB_z &= (A + jB)H(f_c) = \sqrt{A^2 + B^2}|H(f_c)|e^{j(\nu + \phi(f_c))} = \\
 &= (A + jB)(H_{Re}(f_c) + jH_{Im}(f_c))
 \end{aligned}
 \tag{3.110}$$

A COMPACT MODEL WITH A COMPLEX CHANNEL PARAMETER!!

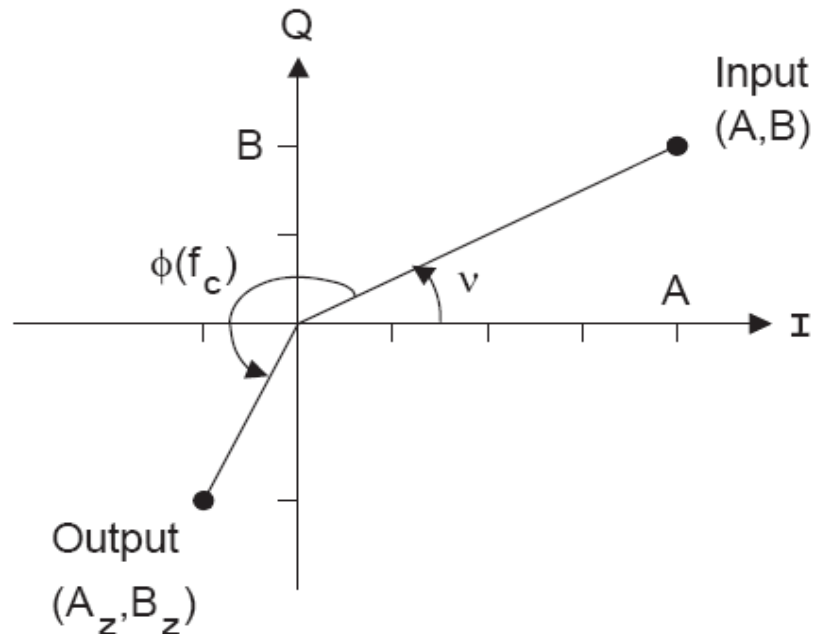


Figure 3.13: Illustrating that the input I-Q amplitudes (A,B) are scaled and rotated by the channel $H(f)$, see (3.109) and (3.110).

$$z(t) = \begin{cases} 0 & , t < 0 \\ \text{“non-stationary transient” starting interval} & , 0 \leq t \leq T_h \\ |H(f_c)|\sqrt{A^2 + B^2} \cos(\omega_c t + \nu + \phi(f_c)) & , T_h \leq t \leq T_s \\ \text{“non-stationary transient” ending interval} & , T_s \leq t \leq T_s + T_h \\ 0 & , t > T_s + T_h \end{cases}$$

and within $T_h \leq t \leq T_s$, $A_z + jB_z = (A + jB)H(f_c)$

(3.111)

An important result here is that the input QAM signal $x(t)$ in (3.106) is changed to a new QAM signal by $|H(f_c)|$ and $\phi(f_c)$ in the interval $T_h \leq t \leq T_s$, see also Figure 3.13 and (3.110) how the I-Q components are changed. Furthermore, in OFDM applications the signaling rate $1/T_s$ is low such that $T_s \gg T_h$, and many QAM signals with different carrier frequencies are sent in parallel. *Due to linearity, the result in (3.111) can be applied to each QAM signal in the OFDM signal by replacing f_c with f_n .* In OFDM applications the receiver uses the time interval $\Delta_h \leq t \leq T_s$ for detection of the output QAM signals, and the duration of this observation interval is denoted $T_{obs} = T_s - \Delta_h$ (compare with (2.110) on page 51, and $T_h \leq \Delta_h$).

So, the n :th QAM signal constellation in a sent OFDM signal is attenuated and rotated by $H(f_n)$ which is the value of the channel transfer function $H(f)$ at the carrier frequency f_n .

3.4.3 N-Ray Channel Model

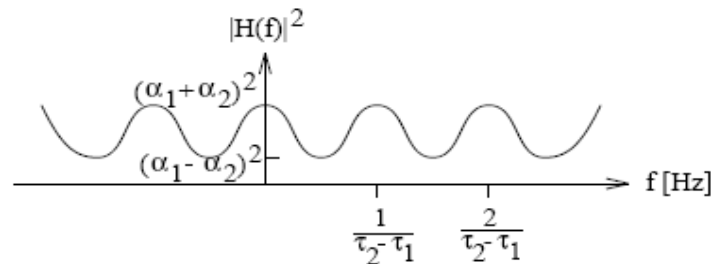
$$z(t) = x(t) * \underbrace{\left(\sum_{i=1}^N \alpha_i \delta(t - \tau_i) \right)}_{\text{Impulse response } h(t)} = \sum_{i=1}^N \alpha_i x(t - \tau_i) \quad (3.126)$$

$$H(f) = \mathcal{F}\{h(t)\} = \sum_{i=1}^N \alpha_i e^{-j2\pi f \tau_i} \quad (3.128)$$

So, $\mathbf{H(f)}$ is easy to find!

EXAMPLE 3.20

Rough sketch:



It is seen in this figure that the two signal paths add constructively or destructively (fading) depending on the frequency. Furthermore, if $\alpha_1 \approx \alpha_2$ then $|H(f)|$ is very close to zero at certain frequencies (so-called deep fades)!

Then (5.135) can be formulated as,

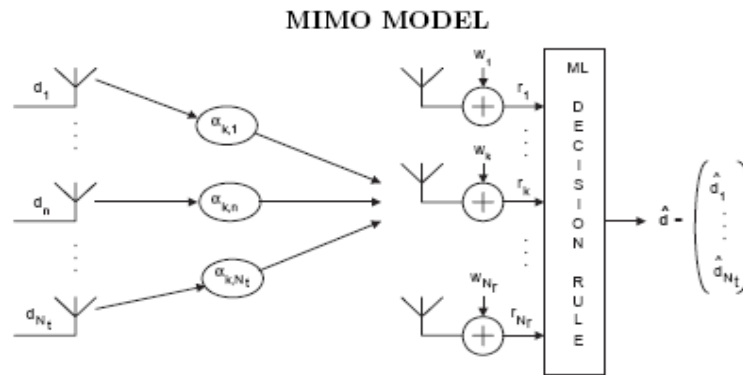
$$r_k = \sum_{n=1}^{N_t} \alpha_{k,n} d_n + w_k, \quad k = 1, 2, \dots, N_r \quad (5.137)$$

A compact formulation is now obtained as

$$\mathbf{r} = \begin{pmatrix} r_1 \\ \vdots \\ r_{N_r} \end{pmatrix} = \mathbf{A} \begin{pmatrix} d_1 \\ \vdots \\ d_{N_t} \end{pmatrix} + \begin{pmatrix} w_1 \\ \vdots \\ w_{N_r} \end{pmatrix} = \mathbf{A}\mathbf{d} + \mathbf{w} \quad (5.138)$$

where the $N_r \times N_t$ matrix \mathbf{A} contains the channel coefficients $\{\alpha_{k,n}\}$. The relationship in (5.138) is a basic model in so-called multiple-input multiple-output (MIMO) systems.

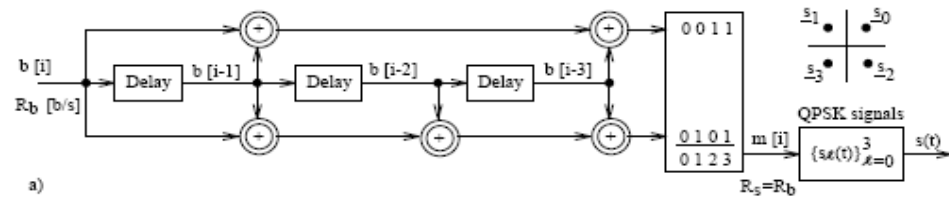
The MIMO model is illustrated in the figure below,



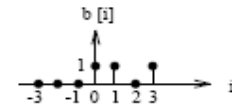
$$r_k = \sum_{n=1}^{N_t} \alpha_{k,n} d_n + w_k$$

$$\mathbf{r} = \begin{pmatrix} r_1 \\ \vdots \\ r_{N_r} \end{pmatrix} = \mathbf{A} \begin{pmatrix} d_1 \\ \vdots \\ d_{N_t} \end{pmatrix} + \begin{pmatrix} w_1 \\ \vdots \\ w_{N_r} \end{pmatrix} = \mathbf{A}\mathbf{d} + \mathbf{w}$$

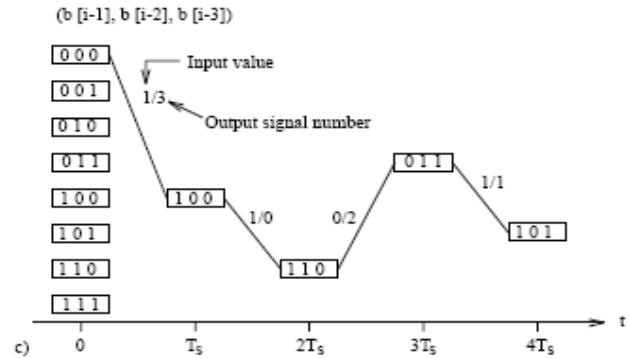
64-QAM+Nt=8 (48bits): ML symbol decision rule



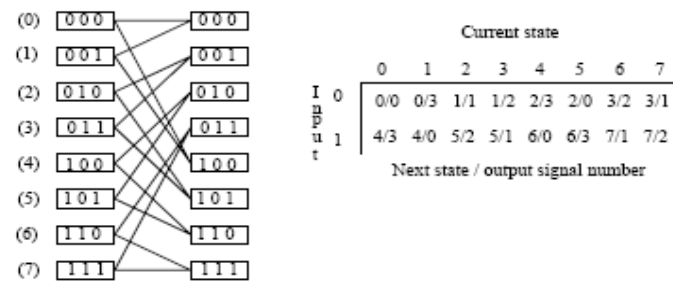
a)



b)

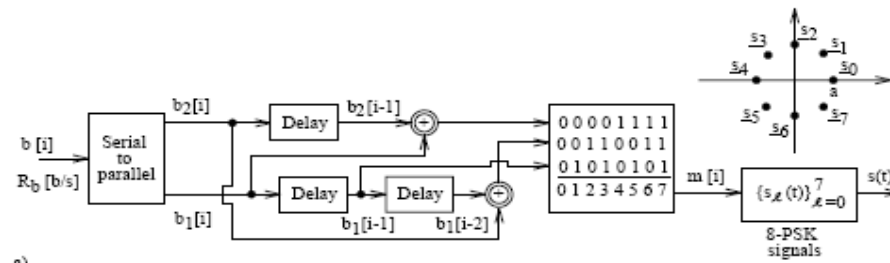


c)



d)

Figure 8.4: a) A rate 1/2 convolutional encoder combined with QPSK signal alternatives; b) A specific input sequence $b[i]$; c) The corresponding path in the trellis; d) A trellis section, and a table containing all relevant parameters.

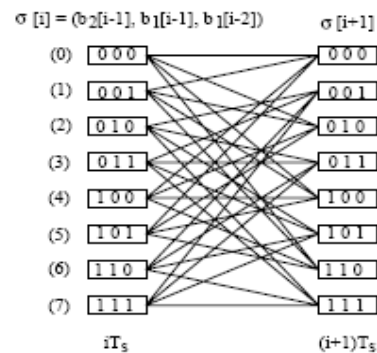


a)

		Current state $\sigma [i]$							
		(000)	(001)	(010)	(011)	(100)	(101)	(110)	(111)
		0	1	2	3	4	5	6	7
$\begin{matrix} \uparrow \\ \text{TCM} \\ \downarrow \end{matrix}$	$\begin{pmatrix} 0 \\ 0 \\ 0 \end{pmatrix}$	0/0	0/2	1/1	1/3	0/4	0/6	1/5	1/7
	$\begin{pmatrix} 0 \\ 0 \\ 1 \end{pmatrix}$	2/4	2/6	3/5	3/7	2/0	2/2	3/1	3/3
	$\begin{pmatrix} 1 \\ 0 \\ 0 \end{pmatrix}$	4/2	4/0	5/3	5/1	4/6	4/4	5/7	5/5
	$\begin{pmatrix} 1 \\ 1 \\ 1 \end{pmatrix}$	6/6	6/4	7/7	7/5	6/2	6/0	7/3	7/1

$\sigma [i+1] / m [i]$

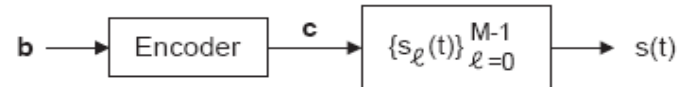
b)



c)

Figure 8.6: a) An example of TCM, from [63]–[64]; b) The mappings $F(\cdot, \cdot)$ and $G(\cdot, \cdot)$; c) A trellis section.

2.32 Let us here study adaptive coding and modulation according to the block diagram below.



$$\bar{E}_{sent} = r_c \log_2(M) E_{b,sent} = \frac{k}{n} \log_2(M) E_{b,sent} \quad (8.4)$$

$$R_s = 1/T_s = \frac{1}{r_c} \cdot \frac{1}{\log_2(M)} \cdot R_b = \frac{1}{k/n} \cdot \frac{1}{\log_2(M)} \cdot R_b \quad (8.5)$$

$$W = c \cdot R_s \quad (8.6)$$

Typically, the bandwidth W is fixed and given but:
the rate of the encoder
the number of signal alternatives
and the bit rate can be **ADAPTIVE**, see (8.5)-(8.6)!

We have memory in the sequence of sent signal alternatives!

Some sequences are impossible, see problem!

Only "good" sequences are sent!

OFDM - INTRO

$$\begin{aligned}
 \text{OFDM signal}(t) &= g_{rec}(t) \sum_{k=0}^{K-1} \text{Re}\{a_k e^{j2\pi f_k t}\} = g_{rec}(t) \text{Re}\{\sum_{k=0}^{K-1} a_k e^{j2\pi f_k t}\} = \\
 &= g_{rec}(t) \text{Re}\{\sum_{k=0}^{K-1} a_k e^{j2\pi(f_0 + kf_\Delta)t}\} = g_{rec}(t) \text{Re}\{(\sum_{k=0}^{K-1} a_k e^{j2\pi(g_0 + k)f_\Delta t}) e^{j2\pi f_{rc} t}\} = \\
 &= g_{rec}(t) \text{Re}\{(\sum_{k=0}^{K-1} a_k e^{j2\pi g_k f_\Delta t}) e^{j2\pi f_{rc} t}\} \tag{1.13}
 \end{aligned}$$

Equation (1.13) shows that an OFDM signal can be viewed as the sum of K QAM signals.

$$a_k = a_{k,I} + ja_{k,Q}, \quad k = 0, 1, \dots, K - 1 \tag{1.5}$$

$$T_{obs} = T_s - T_{CP} \tag{1.18}$$

$$f_\Delta = 1/T_{obs} \tag{2.1}$$

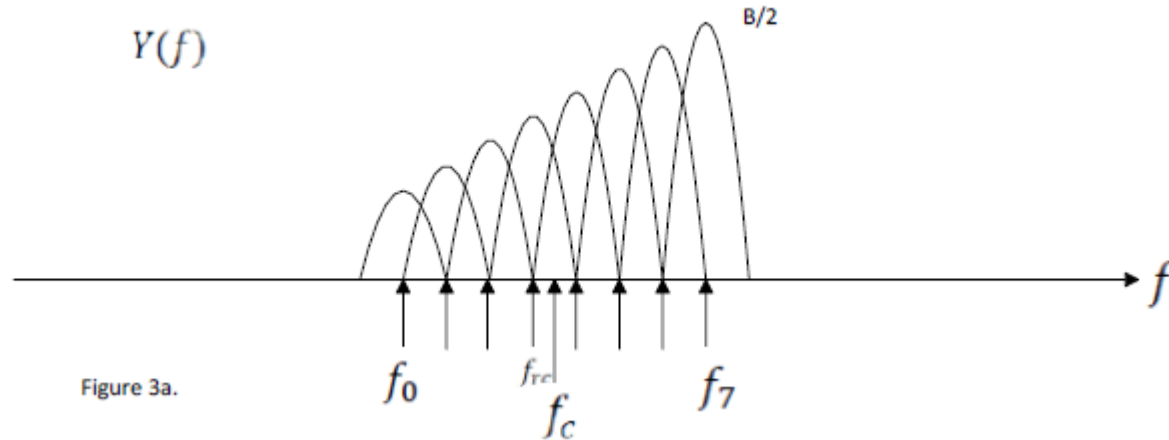


Figure 3a.

$$f_k = f_0 + kf_\Delta, \quad k = 0, 1, \dots, K - 1 \quad (1.1)$$

$$W_{OFDM} \approx Kf_\Delta \text{ (Hz)} \quad (1.3)$$

The transmitted *information bit rate*, denoted R_b , then equals,

$$R_b = \frac{r_c \sum_{k=0}^{K-1} \log_2(M_k)}{T_s} \text{ (bps)} \quad (1.16)$$

Furthermore, assuming also that K is $\gg 1$ the *bandwidth efficiency*, denoted ρ , is

$$\rho = \frac{R_b}{W_{OFDM}} = \frac{r_c \sum_{k=0}^{K-1} \log_2(M_k)}{T_s K f_\Delta} \text{ (bps/Hz)} \quad (1.17)$$

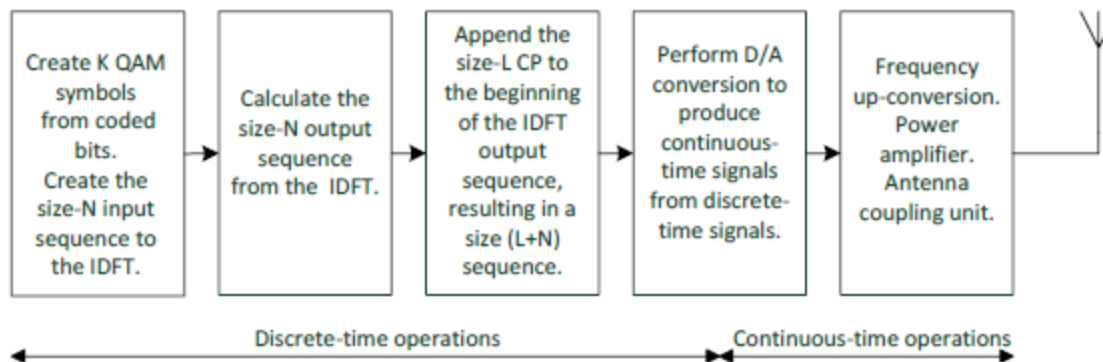


Figure 1. Illustrates the over-all structure and operations performed by an OFDM transmitter within an OFDM symbol interval T_s .

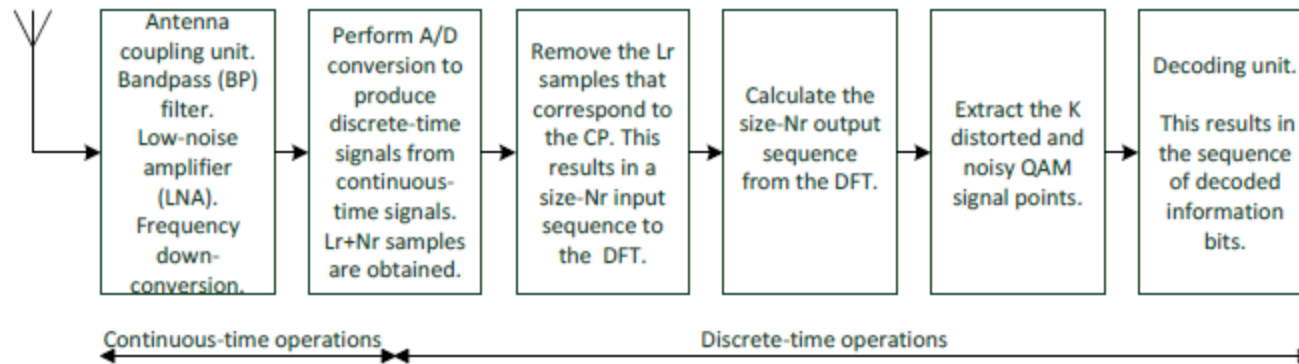


Figure 2. Illustrates the over-all structure and operations performed by an OFDM receiver within an OFDM symbol interval T_s .

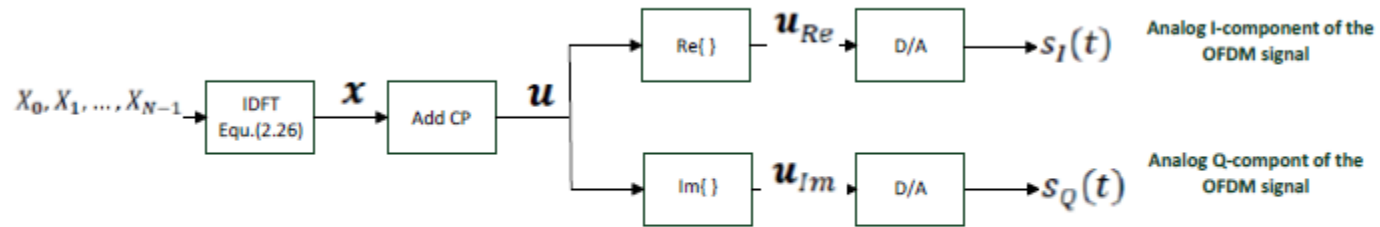


Figure 7. Block diagram illustrating the operations in the digital domain, and the transition to the analog domain.

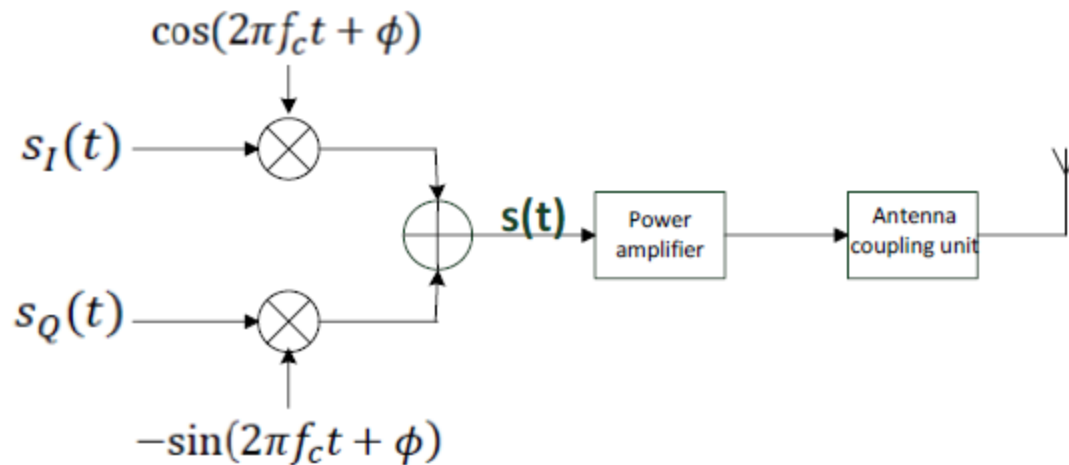


Figure 8. Block diagram illustrating frequency up-conversion (mixer stage) to the carrier frequency (K is odd), the power amplifier, and the antenna coupling unit. The OFDM signal $s(t)$ is given in equation (4.1).

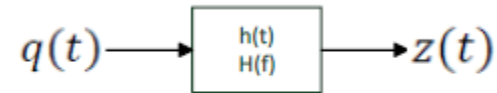


Figure 9. Illustrating a linear time-invariant filter channel.

$$\text{INPUT OFDM: } A_s(t) = A \operatorname{Re}\left\{\sum_{n=0}^{K-1} a_n e^{j(2\pi f_n t + \theta_n)}\right\}, \quad 0 \leq t \leq T_s$$

$$\text{OUTPUT OFDM: } z(t) = A \operatorname{Re}\left\{\sum_{n=0}^{K-1} a_n H(f_n) e^{j(2\pi f_n t + \theta_n)}\right\}, \quad T_{CP} \leq t \leq T_s \quad (5.13)$$

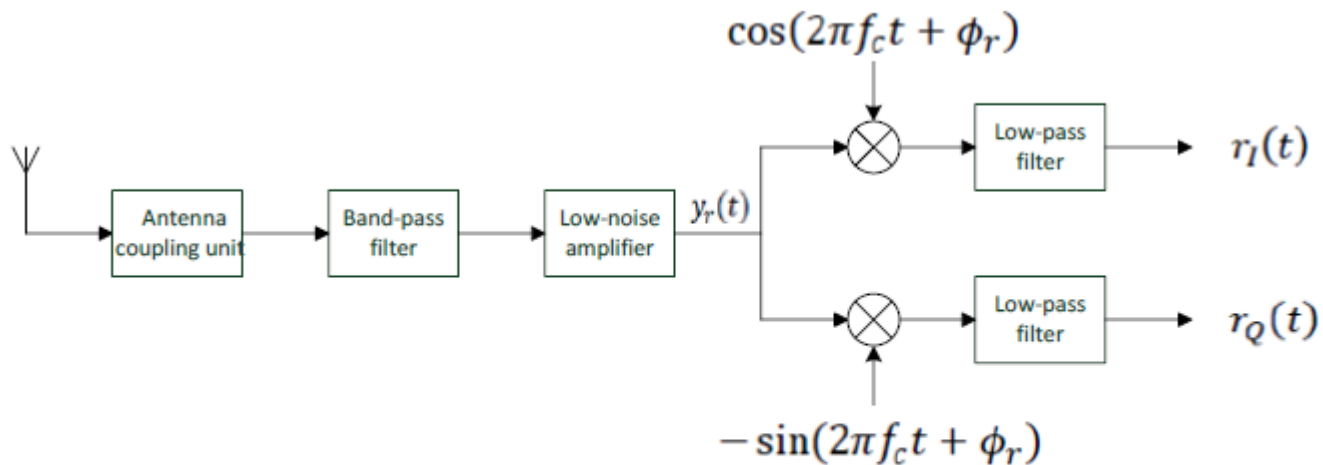


Figure 10. Illustrating the first part of the receiver: the antenna coupling unit, band-pass filter (wide), low-noise amplifier (LNA) and a homodyne unit for frequency down-conversion and extracting the baseband signals $r_I(t)$ and $r_Q(t)$. It is here assumed that K is odd for which $f_{rc} = f_c$.

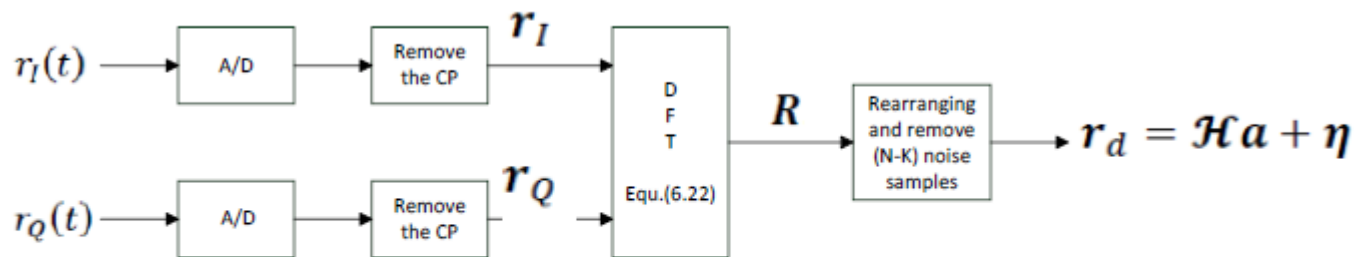


Figure 11. Illustrating sampling, removal of the CP, and the size- N DFT in the receiver to extract the K received distorted and noisy signal points collected in the size- K vector r_d .

$$\begin{aligned}
\text{OFDM signal}(t) &= g_{rec}(t) \sum_{k=0}^{K-1} \text{Re}\{a_k e^{j2\pi f_k t}\} = g_{rec}(t) \text{Re}\{\sum_{k=0}^{K-1} a_k e^{j2\pi f_k t}\} = \\
&= g_{rec}(t) \text{Re}\{\sum_{k=0}^{K-1} a_k e^{j2\pi(f_0+kf_\Delta)t}\} = g_{rec}(t) \text{Re}\{(\sum_{k=0}^{K-1} a_k e^{j2\pi(g_0+k)f_\Delta t}) e^{j2\pi f_{rc} t}\} = \\
&= g_{rec}(t) \text{Re}\{(\sum_{k=0}^{K-1} a_k e^{j2\pi g_k f_\Delta t}) e^{j2\pi f_{rc} t}\} \tag{1.13}
\end{aligned}$$

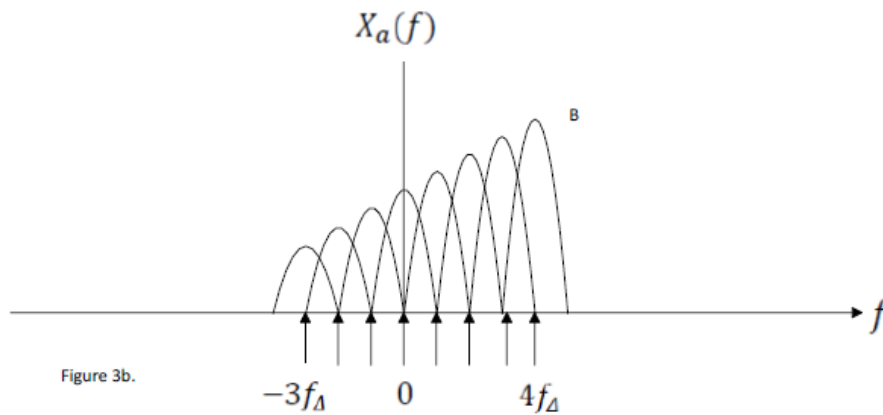
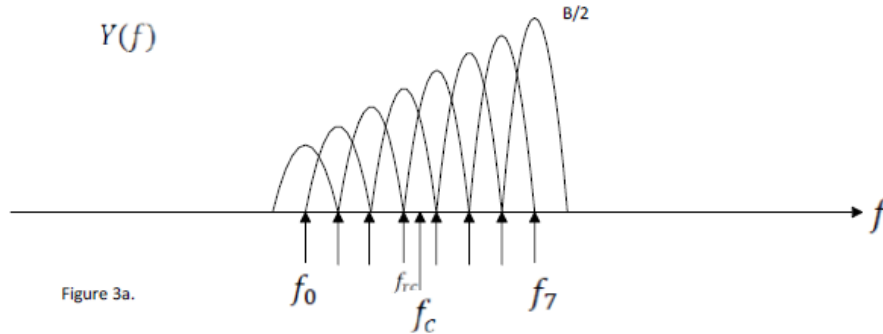
$$f_k = f_{rc} + g_k f_\Delta, \quad k = 0, 1, \dots, K-1 \tag{1.8}$$

The numbers g_k range from g_0 to g_{K-1} ,

$$g_k: -\frac{K-1}{2} = g_0, \dots, -1, 0, 1, \dots, \frac{K-1}{2} = g_{K-1} \quad \text{if } K \text{ is odd} \tag{1.11}$$

$$g_k: -\frac{K-2}{2} = g_0, \dots, -1, 0, 1, \dots, \frac{K}{2} = g_{K-1} \quad \text{if } K \text{ is even} \tag{1.12}$$

$$y(t) = \text{Re}\left\{\left(\sum_{k=0}^{K-1} a_k e^{j2\pi g_k f \Delta t}\right) e^{j2\pi f_{rc} t}\right\} = \text{Re}\{x(t) e^{j2\pi f_{rc} t}\} \quad (2.2)$$



$$x(t) = x_{Re}(t) + jx_{Im}(t) = \sum_{k=0}^{K-1} a_k e^{j2\pi g_k f \Delta t}, \quad 0 \leq t \leq T_{obs} \quad (2.3)$$

Observe in Equation (2.3) that the QAM symbol a_k ($k=0,1,\dots,(K-1)$), is carried by the baseband sub-carrier frequency $g_k f_{\Delta}$ in the complex baseband OFDM signal $x(t)$!

The high-frequency OFDM signal $y(t)$ in Equation (2.2) can be written as,

$$y(t) = \text{Re}\{x(t)e^{j2\pi f_{rc}t}\} = x_{\text{Re}}(t) \cos(2\pi f_{rc}t) - x_{\text{Im}}(t) \sin(2\pi f_{rc}t) \quad (2.5)$$

Equation (2.5) is an important relationship since it shows that the OFDM-signal $y(t)$ is *easily implemented* as soon as we have created the real part $x_{\text{Re}}(t)$ and the imaginary part $x_{\text{Im}}(t)$ of $x(t)$.

We should therefore focus on creating $x(t)$, since $x_{\text{Re}}(t)$ and $x_{\text{Im}}(t)$ then are easy to find.

Let us now sample the complex signal $x(t)$ in Equation (2.3) every $\frac{T_{obs}}{N}$ second, i.e. with N samples within the time-interval $0 \leq t < T_{obs}$. This corresponds to a sampling frequency f_{samp} equal to,

$$f_{samp} = N/T_{obs} = Nf_{\Delta} > Kf_{\Delta} \quad (2.12)$$

samples per second, and N should be chosen larger than K , and large enough such that the sampling theorem can be considered to be sufficiently fulfilled.

$$x_n = x(nT_{obs}/N) = \sum_{k=0}^{K-1} a_k e^{j2\pi g_k n/N} \quad n = 0, 1, \dots, (N-1) \quad (2.13)$$

Observe that the right hand side of equation (2.13) actually gives us a way to create the desired samples x_0, x_1, \dots, x_{N-1} of the complex baseband OFDM signal $x(t)$!

the Fourier transform $X(v)$ of the discrete-time signal x in Equation (2.13). $X(v)$ is defined by, see ref. [1],

$$X(v) = \sum_{n=0}^{N-1} x_n e^{-j2\pi v n} \quad (2.14)$$

Note in Equation (2.14) that the Fourier transform $X(v)$ is periodic in v with period 1. Furthermore, the variable v can be viewed as a **normalized frequency variable**, $v = f/f_{samp}$. The periodicity in v is illustrated in Figure 4 on the next page.

$$x_n = x(nT_{obs}/N) = \sum_{k=0}^{K-1} a_k e^{j2\pi g_k n/N} \quad n = 0, 1, \dots, (N-1) \quad (2.13)$$

$$X(v) = \sum_{n=0}^{N-1} x_n e^{-j2\pi v n} \quad (2.14)$$

Furthermore, let X_m denote the **frequency-domain sample** of $X(v)$ at $v = m/N$, defined by

$$X_m = X(v = m/N) = \sum_{n=0}^{N-1} x_n e^{-j2\pi m n/N}, \quad m = 0, 1, \dots, N-1 \quad (\text{DFT}) \quad (2.15)$$

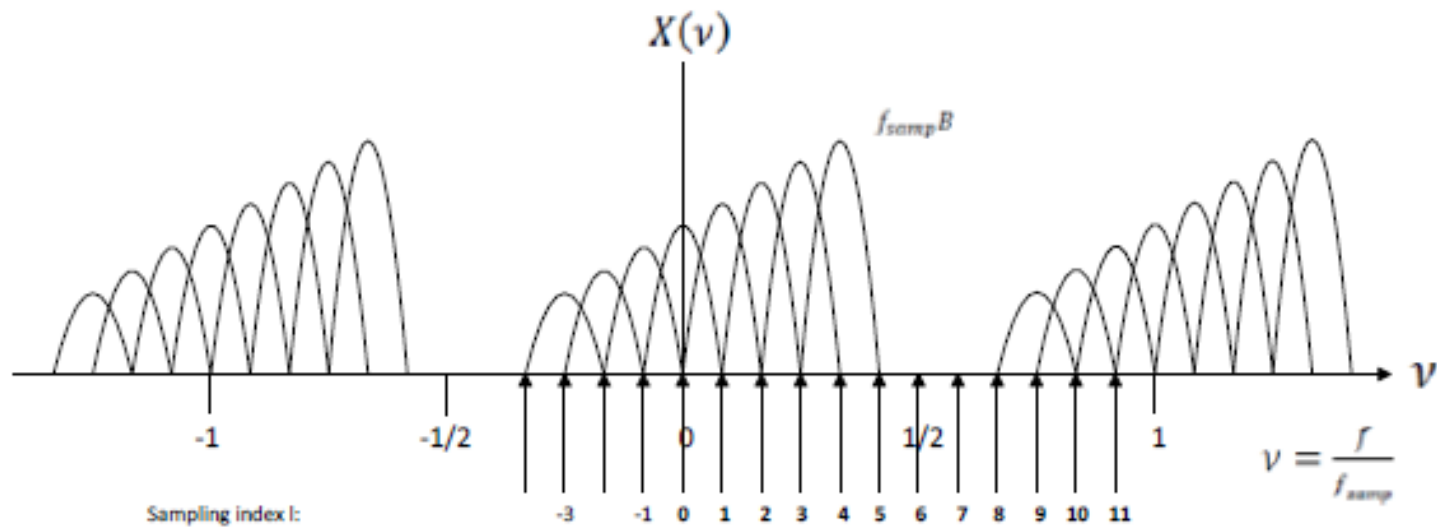
This is the definition (see ref. [1]) of the size- N **DFT** (Discrete Fourier Transform) of the sequence x .

However, for the moment we are particularly interested in the size- N **IDFT** (Inverse Discrete Fourier transform) which is defined by (see ref. [1]),

$$x_n = \frac{1}{N} \sum_{m=0}^{N-1} X_m e^{j2\pi m n/N}, \quad n = 0, 1, \dots, N-1 \quad (\text{IDFT}) \quad (2.16)$$

Hence, as soon as we have determined the samples in the frequency domain X_0, X_1, \dots, X_{N-1} we should use them in the size- N IDFT in Equation (2.16) to create the desired sequence of time-domain samples x ! The values X_m will be determined in step 3.

In practice, N is chosen to be a power of 2 since fast Fourier transform (FFT) algorithms then can be used to significantly speed up the calculations in Equations (2.15) - (2.16).



$$X(v) = \sum_{n=0}^{N-1} x_n e^{-j2\pi v n} \quad (2.14)$$

$$X_m = X(v = m/N) = \sum_{n=0}^{N-1} x_n e^{-j2\pi m n / N}, \quad m = 0, 1, \dots, N-1 \quad (\text{DFT}) \quad (2.15)$$

$$x_n = \frac{1}{N} \sum_{m=0}^{N-1} X_m e^{j2\pi m n / N}, \quad n = 0, 1, \dots, N-1 \quad (\text{IDFT}) \quad (2.16)$$

Consider as an **example** the case $K=8$ and $N=12$. In this case $k_{rc} = 3$ and $g_{K-1} = 4$, and the desired sequence X_0, X_1, \dots, X_{11} then equals: $Na_3, Na_4, Na_5, Na_6, Na_7, 0, 0, 0, 0, Na_0, Na_1, Na_2$. See also Figure 6.

Step 3: The relation between the sequences a_0, a_1, \dots, a_{K-1} and X_0, X_1, \dots, X_{N-1} .

Let us use Equation (2.13) to establish the connection between the sequences a_0, a_1, \dots, a_{K-1} and X_0, X_1, \dots, X_{N-1} . We rewrite Equation (2.13) in the following way,

$$\begin{aligned}
 x_n &= x\left(\frac{nT_{obs}}{N}\right) = \sum_{k=0}^{K-1} a_k e^{\frac{j2\pi g_k n}{N}} = \sum_{k=0}^{K-1} a_k e^{j2\pi(g_0+k)n/N} = \\
 &= \sum_{k=0}^{-g_0-1} a_k e^{j2\pi(g_0+k+N)n/N} + \sum_{k=-g_0}^{K-1} a_k e^{j2\pi(g_0+k)n/N} = \\
 &= \sum_{m=g_0+N}^{N-1} a_{m-(g_0+N)} e^{j2\pi mn/N} + \sum_{m=0}^{g_{K-1}} a_{m-g_0} e^{j2\pi mn/N} = \\
 &= \frac{1}{N} \sum_{m=0}^{N-1} X_m e^{j2\pi mn/N} \tag{2.18}
 \end{aligned}$$

Inspection of Equation (2.18) yields the relationships below:

$$X_m = Na_{m-g_0}, \quad \text{if } 0 \leq m \leq g_{K-1} \tag{2.19}$$

$$X_m = 0, \quad \text{if } g_{K-1} + 1 \leq m \leq g_0 + N - 1 \tag{2.20}$$

$$X_m = Na_{m-(g_0+N)}, \text{ if } g_0 + N \leq m \leq N - 1 \tag{2.21}$$

The last expression in Equation (2.18) is identical to the size-N IDFT in Equation (2.16). The relation between the sequences a_0, a_1, \dots, a_{K-1} and X_0, X_1, \dots, X_{N-1} are given by Equations (2.19) – (2.21).

$$X_l = Na_{k_{rc}+l} \quad l = 0, 1, \dots, g_{K-1} \quad (2.27)$$

$$X_{-k_{rc}+N+k} = Na_k \quad k = 0, 1, \dots, (k_{rc} - 1) \quad (2.29)$$

If we first construct the size-N sequence $Na_0, Na_1, \dots, Na_{K-1}, 0, 0, \dots, 0$, and then “left-rotate” this sequence n_{rc} positions (or “right-rotate” this sequence $(g_0 + N)$ positions), then the desired sequence X_0, X_1, \dots, X_{N-1} in equations (2.20)-(2.25) is obtained!

Consider as an **example** the case $K=8$ and $N=12$. In this case $k_{rc} = 3$ and $g_{K-1} = 4$, and the desired sequence X_0, X_1, \dots, X_{11} then equals: $Na_3, Na_4, Na_5, Na_6, Na_7, 0, 0, 0, 0, Na_0, Na_1, Na_2$. See also Figure 6.

The final step is to calculate the size- N **IDFT**,

$$x_n = \frac{1}{N} \sum_{m=0}^{N-1} X_m e^{j2\pi mn/N}, \quad n = 0, 1, \dots, N - 1 \quad (2.30)$$

In practice, N is chosen to be a power of 2 since fast Fourier transform (FFT) algorithms can then be used to significantly speed up the calculations in equation (2.30).

Equation (2.30) is the desired final expression to compute the discrete-time signal x , i.e. the N time-domain samples of the complex baseband OFDM signal $x(t)$. Equation (2.30), i.e. the size- N IDFT, is computationally very efficient when implemented using FFT algorithms (if N is chosen to be a power of 2). The sequence X_0, X_1, \dots, X_{N-1} is given by Equations (2.27) and (2.29) or alternatively by Equations (2.19)-(2.21). See also the construction (“rotation”) given above. See also Figure 7 on page 27.

The $(N - K)$ zeroes in the sequence X_0, X_1, \dots, X_{N-1} may be interpreted as using zero-valued signal-points at baseband sub-carrier frequencies located at the edges but outside of the OFDM frequency band.

3. The Cyclic Prefix (CP) and Digital-to-Analog (D/A) conversion

Based on the discussion about periodicity above let us therefore construct a new size-(L+N) vector \mathbf{u} as a so-called *periodic extension* of the size-N vector \mathbf{x} . This means that *the L last samples in \mathbf{x} are copied and placed as the first L samples in \mathbf{u}* . The remaining N samples in \mathbf{u} are identical to \mathbf{x} . This means that,

$$u_0 = x_{N-L}, \dots, u_{L-1} = x_{N-1}, u_L = x_0, \dots, u_{L+N-1} = x_{N-1}. \quad (3.1)$$

The construction of the vector \mathbf{u} above implies that the first L samples in \mathbf{u} are identical with the last L samples in \mathbf{u} , and this reflects the periodicity discussed above.

The duration of the OFDM signal interval is T_s , and it can be expressed as,

$$T_s = \frac{(L+N)T_{obs}}{N} = T_{CP} + T_{obs} \quad (3.2)$$

The vector \mathbf{u} in equation (3.1) contains $(L+N)$ time-domain complex samples of a complex baseband OFDM signal defined over the entire OFDM signal interval $0 \leq t \leq T_s$. This complex baseband OFDM signal is here denoted $\mathbf{u}(t)$, and based on the previous discussion in this section, the OFDM signal $\mathbf{u}(t)$ is,

$$u(t) = u_{Re}(t) + ju_{Im}(t) = \sum_{k=0}^{K-1} a_k e^{j2\pi g_k f_{\Delta}(t-T_{CP})}, \quad 0 \leq t \leq T_s \quad (3.3)$$

$$s(t) = \text{Re}\{u(t)e^{j2\pi f_{rc}t}\} = u_{Re}(t) \cos(2\pi f_{rc}t) - u_{Im}(t) \sin(2\pi f_{rc}t) \quad (3.5)$$

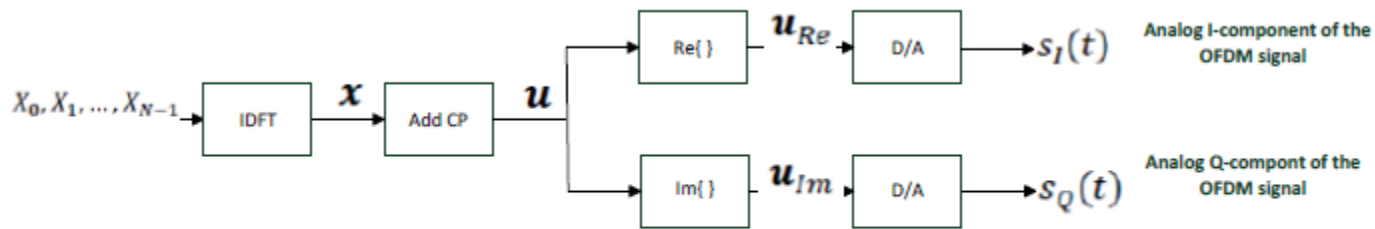


Figure 7. Block diagram illustrating the operations in the digital domain, and the transition to the analog domain. The IDFT is given in Equation (2.30) (and in Equation (2.18)).

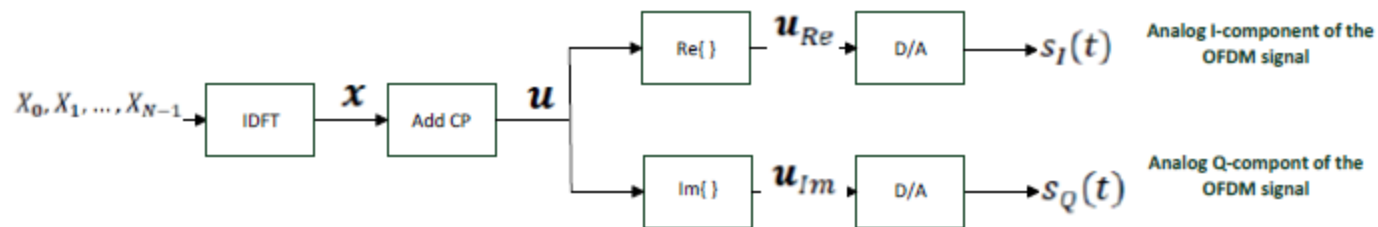


Figure 7. Block diagram illustrating the operations in the digital domain, and the transition to the analog domain. The IDFT is given in Equation (2.30) (and in Equation (2.18)).

$$s(t) = s_I(t) \cos(2\pi f_{rc}t + \phi) - s_Q(t) \sin(2\pi f_{rc}t + \phi) \quad (4.1)$$

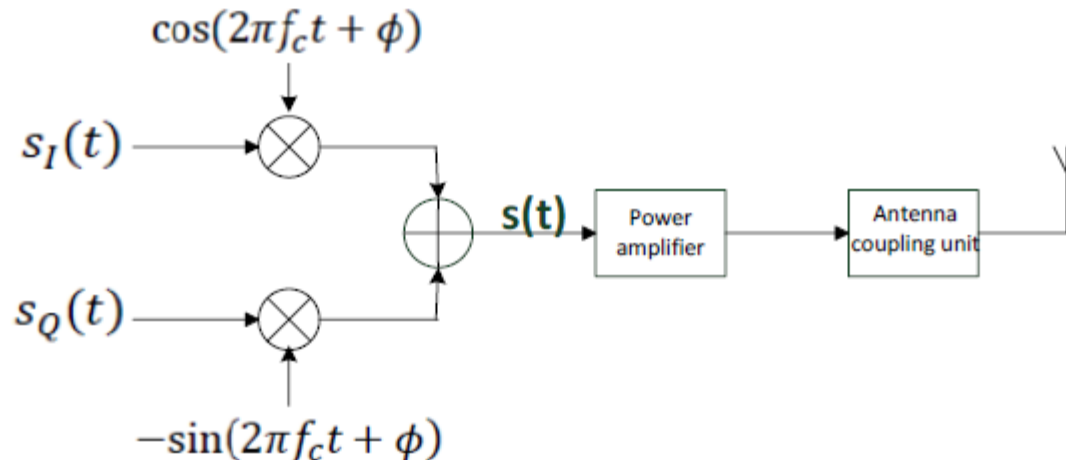


Figure 8. Block diagram illustrating frequency up-conversion (mixer stage) to the carrier frequency (K is odd), the power amplifier, and the antenna coupling unit. The OFDM signal $s(t)$ is given in Equation (4.1).

Section 5: The multi-path (linear filter) channel, and the additive white Gaussian noise (AWGN)

$$\text{INPUT OFDM: } A_s(t) = ARe\left\{\left(\sum_{k=0}^{K-1} a_k e^{j2\pi g_k f_\Delta(t-T_{CP})}\right) e^{j(2\pi f_{rc}t+\phi)}\right\}, \quad 0 \leq t \leq T_s \quad (5.10)$$

or alternatively as,

$$\text{INPUT OFDM: } A_s(t) = ARe\left\{\sum_{k=0}^{K-1} a_k e^{j(2\pi f_k t+\theta_k)}\right\}, \quad 0 \leq t \leq T_s \quad (5.11)$$

$$\text{OUTPUT OFDM: } z(t) = ARe\left\{\left(\sum_{k=0}^{K-1} a_k H(f_k) e^{j2\pi g_k f_\Delta(t-T_{CP})}\right) e^{j(2\pi f_{rc}t+\phi)}\right\}, \quad T_{CP} \leq t \leq T_s \quad (5.12)$$

or alternatively as,

$$\text{OUTPUT OFDM: } z(t) = ARe\left\{\sum_{k=0}^{K-1} a_k H(f_k) e^{j(2\pi f_k t+\theta_k)}\right\}, \quad T_{CP} \leq t \leq T_s \quad (5.13)$$

6. The Receiver: Frequency down-converting, sampling (A/D) and the DFT

$$r(t) = b_I \cos(2\pi f_B t) - b_Q \sin(2\pi f_B t) + n(t), \quad 0 \leq t \leq T$$

$$\psi_1(t) = \cos(2\pi f_B t)/C, \quad 0 \leq t \leq T$$

$$\psi_2(t) = -\sin(2\pi f_B t)/C, \quad 0 \leq t \leq T$$

$$r_1 = \int_0^T r(t)\psi_1(t) dt = Cb_I + n_1 \quad r_2 = \int_0^T r(t)\psi_2(t) dt = Cb_Q + n_2$$

$$r = r_1 + jr_2 = \int_0^T r(t)e^{-j2\pi f_B t} dt/C = R(f_B)/C = Cb + n \quad (6.8)$$

It is now very important to observe in equation (6.8) that the received noisy signal point r can be found by calculating the Fourier transform $R(f)$ of the received signal $r(t)$ over the time interval $0 \leq t \leq T$, and then sample $R(f)$ at $f = f_B$ to obtain $R(f_B)$. As will be seen later on, using the DFT in an OFDM receiver can be viewed as a natural extension of this result. This concludes the example, and it is time to focus on frequency down-converting to baseband.

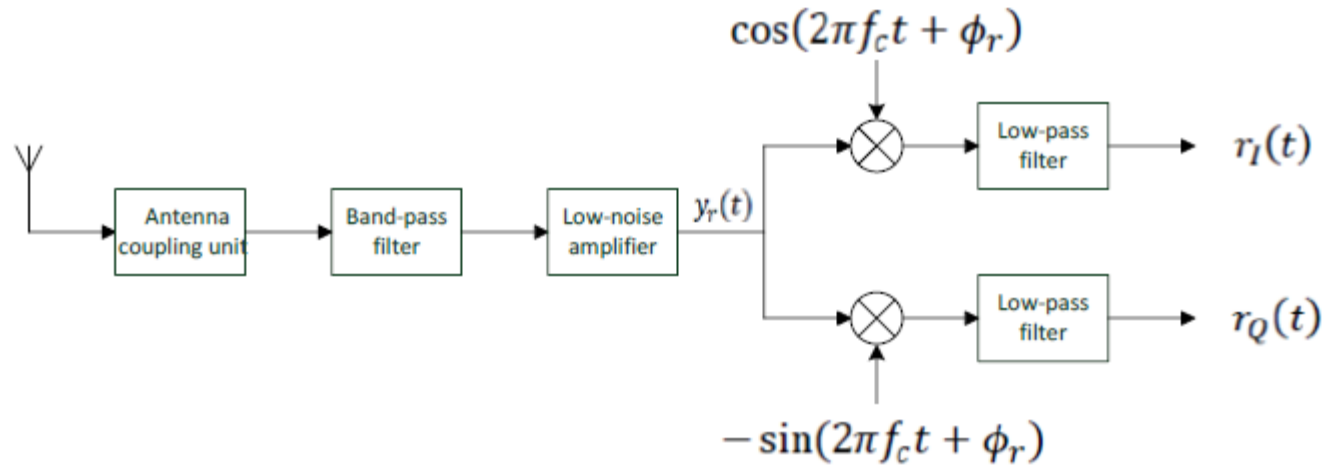


Figure 10. Illustrating the first part of the receiver: the antenna coupling unit, band-pass filter, low-noise amplifier (LNA) and a homodyne unit for frequency down-conversion and extracting the baseband signals $r_I(t)$ and $r_Q(t)$. It is here assumed that K is odd for which $f_{rc} = f_c$.

$$r_I(t) + jr_Q(t) = \sum_{k=0}^{K-1} a_k H_{eq}(f_k) e^{j2\pi g_k f_\Delta (t - T_{CP})} + w(t), \quad T_{CP} \leq t \leq T_s \quad (6.15)$$

$$H_{eq}(f_k) = H_{eq,k} = AH(f_k) e^{j\phi} G_1(f_k) e^{-j\phi_r} G_{lp}(f_k - f_{rc} = g_k f_\Delta) / 2 \quad (6.16)$$

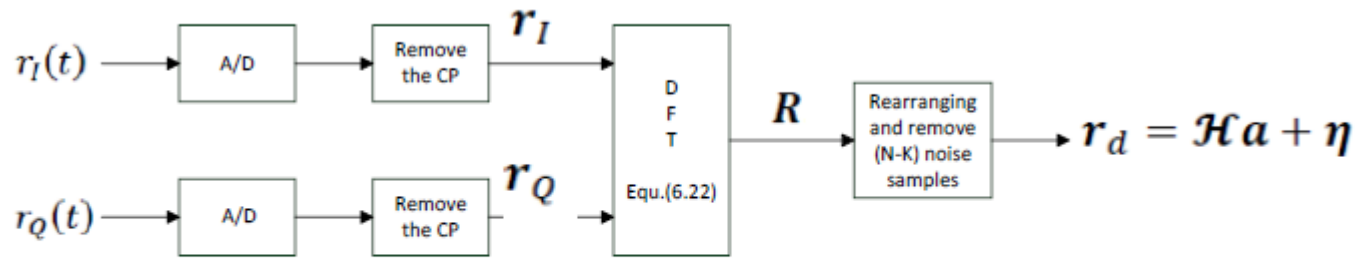


Figure 11. Illustrating sampling, removal of the CP, and the size- N DFT in the receiver to extract the K received distorted and noisy signal points collected in the size- K vector r_d .

$$r_{I,n} = r_I((L + n)T_{obs}/N), \quad n = 0, 1, \dots, N - 1 \quad (6.17)$$

$$r_{Q,n} = r_Q((L + n)T_{obs}/N), \quad n = 0, 1, \dots, N - 1 \quad (6.18)$$

$$\mathbf{r} = \mathbf{r}_I + j\mathbf{r}_Q \quad (6.19)$$

$$R(v) = \sum_{n=0}^{N-1} r_n e^{-j2\pi v n} \quad (6.21)$$

$$R_m = R(v = m/N) = \sum_{n=0}^{N-1} r_n e^{-j2\pi m n / N}, \quad m = 0, 1, \dots, N - 1 \quad (6.22)$$

$$\mathbf{R} = \mathbf{X}_r + \mathbf{w}_r \quad (6.24)$$

$$(\mathcal{H}\mathbf{a})^{tr} = (a_0 H_{eq,0} \ a_1 H_{eq,1} \ \dots \ a_{K-1} H_{eq,K-1}) \quad (6.25)$$

$$\mathbf{X}_r = N\mathbf{Q}_t \mathcal{H}\mathbf{a} \quad (6.26)$$

$$\mathbf{r}_d = \frac{1}{N} \mathbf{Q}_r \mathbf{R} = \mathbf{Q}_r \mathbf{Q}_t \mathcal{H}\mathbf{a} + \frac{1}{N} \mathbf{Q}_r \mathbf{w}_r = \mathcal{H}\mathbf{a} + \boldsymbol{\eta} \quad (6.28)$$

Observe that the elements in the size- K column vector \mathbf{r}_d in Equation (6.28) are the desired received distorted and noisy signal points,

$$r_{d,k} = a_k H_{eq,k} + \eta_k, \quad k = 0, 1, \dots, (K - 1) \quad (6.29)$$

The results in Equations (6.28)-(6.29) are extremely important!

For the special case of *uncoded* OFDM (though rarely used in practice)

$$P_{s,k} = 4 \left(1 - \frac{1}{\sqrt{M_k}}\right) Q \left(\sqrt{\frac{d_{min,k}^2 \mathcal{E}_{b,k}}{N'_{0,k}}} \right) - 4 \left(1 - \frac{1}{\sqrt{M_k}}\right)^2 Q^2 \left(\sqrt{\frac{d_{min,k}^2 \mathcal{E}_{b,k}}{N'_{0,k}}} \right), \quad k = 0, 1, \dots, K - 1 \quad (6.30)$$

where $d_{min,k}^2$ is the normalized squared minimum Euclidean distance in the received QAM signal constellation with index k and,

$$d_{min,k}^2 = \frac{3 \log_2(M_k)}{M_k - 1} \quad (6.31)$$

Furthermore, $\mathcal{E}_{b,k}$ denotes the average received signal energy per information bit in the received QAM signal space with index k , and $\mathcal{E}_{b,k}$ is proportional to $|H_{eq,k}|^2$. The variance of the noise, in each dimension in the two-dimensional signal space with index k , is here $N'_{0,k}/2$.

Chapter 9

An Introduction to Time-varying Multipath Channels

$$z(t) = \sum_n \alpha_n(t) s(t - \tau_n(t)) \quad (9.1)$$

Chapter 9

An Introduction to Time-varying Multipath Channels

$$z(t) = \sum_n \alpha_n(t) s(t - \tau_n(t)) \quad (9.1)$$

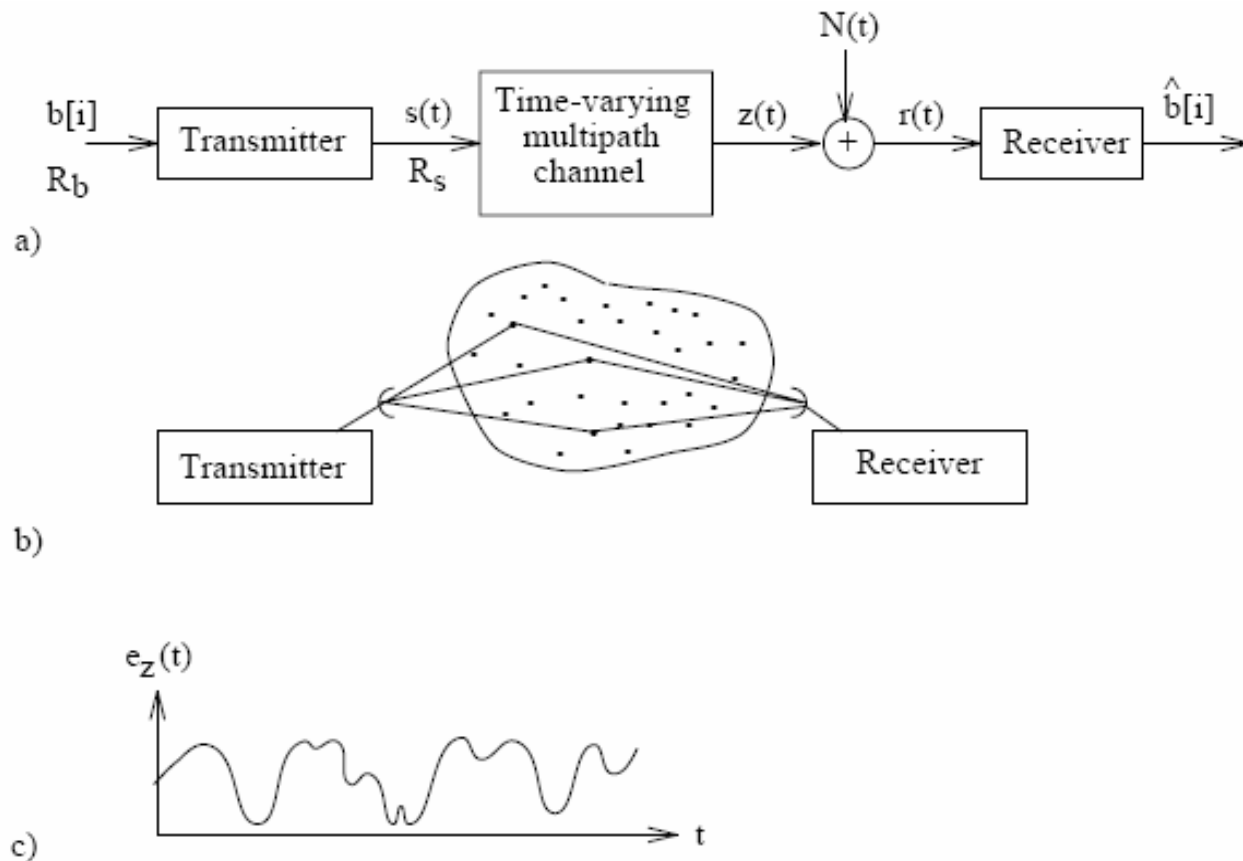
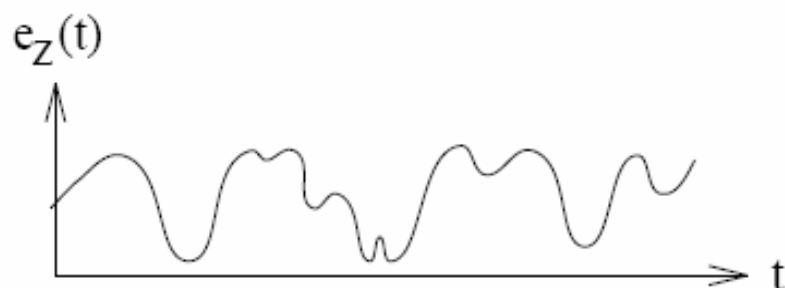


Figure 9.1: a) The digital communication system; b) A scattering medium; c) Illustrating the fading envelope $e_z(t)$.

$$s(t) = \cos((\omega_c + \omega_1)t) , \quad -\infty \leq t \leq \infty \quad (9.2)$$

$$\begin{aligned} z(t) &= \sum_n \alpha_n(t) \cos((\omega_c + \omega_1)(t - \tau_n(t))) = \\ &= e_z(t) \cos((\omega_c + \omega_1)t + \theta_z(t)) \end{aligned} \quad (9.3)$$



Observe that the quadrature components $z_I(t)$ and $z_Q(t)$ in (9.3) are *time-varying*. Hence, the output signal $z(t)$ is *not* a pure sine wave with frequency $f_c + f_1$. *This is a significant difference compared with the linear time-invariant channel.* It is seen in (9.3) that the quadrature components depend

9.1.1 Doppler Power Spectrum and Coherence Time

$$\begin{aligned}
 R_{\mathcal{D}}(f) &= \mathcal{F}(\tilde{c}_z(\tau)) \\
 \tilde{c}_z(\tau) &= \frac{1}{2} E\{[z_I(t+\tau) + jz_Q(t+\tau)] [z_I(t) - jz_Q(t)]\} \\
 R_z(f) &= \frac{1}{2} (R_{\mathcal{D}}(f + f_c + f_1) + R_{\mathcal{D}}(f - f_c - f_1))
 \end{aligned}
 \tag{9.7}$$

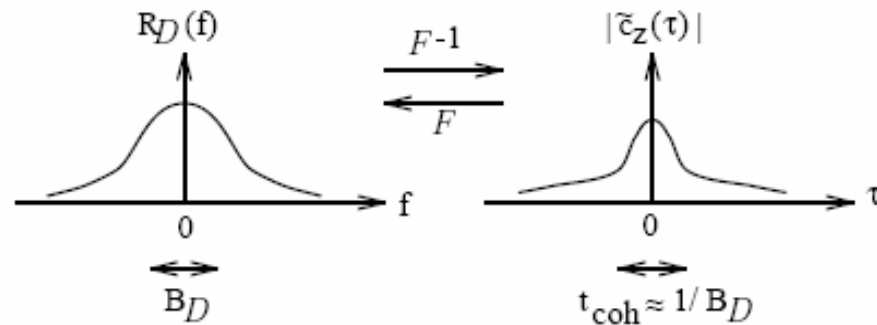


Figure 9.2: Illustrating the Fourier transform pair $\tilde{c}_z(\tau) \longleftrightarrow R_{\mathcal{D}}(f)$.

$$t_{coh} \approx 1/B_{\mathcal{D}}
 \tag{9.8}$$

9.1.2 Coherence Bandwidth and Multipath Spread

$$z(t) = z(f_1, t) = \underbrace{\frac{1}{2} \tilde{H}_{Re}(f_1, t)}_{z_I(t)} \cos((\omega_c + \omega_1)t) - \underbrace{\frac{1}{2} \tilde{H}_{Im}(f_1, t)}_{z_Q(t)} \sin((\omega_c + \omega_1)t) \quad (9.9)$$

What can be said about the output signal $z(t)$ if another frequency $f_2 = f_1 + f_\Delta$ is used, instead of f_1 ? Are different frequency-intervals, in the input signal spectrum, treated differently by the time-varying multipath channel? To answer these questions the correlation between $z(f_1, t)$ and $z(f_1 + f_\Delta, t)$ can be found by

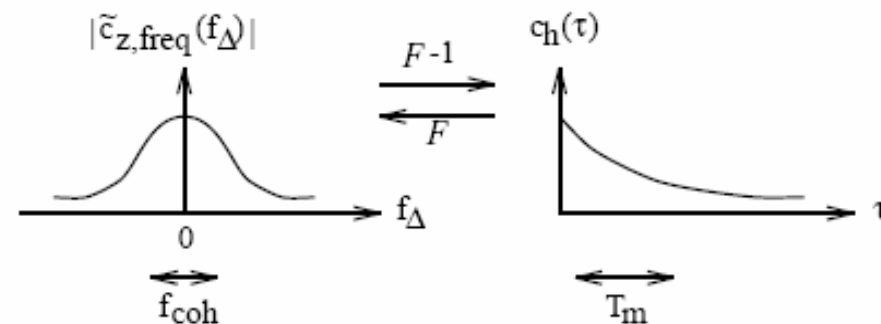


Figure 9.3: Illustrating the Fourier transform pair $c_h(\tau) \longleftrightarrow \tilde{c}_{z, \text{freq}}(f_\Delta)$.

9.2 Frequency-Nonselective, Slowly Fading Channel

$$T_s \ll t_{coh} \quad (9.27)$$

or equivalently,

$$B_{\mathcal{D}} \ll R_s \quad (9.28)$$

This means that the channel is **slowly fading**, which imply that it can be treated as a time-invariant channel within the coherence time.

In this subsection a frequency-nonselective channel is investigated. To obtain this situation it is required that the bandwidth of the transmitted signal, denoted W , is much smaller than the coherence bandwidth f_{coh} of the channel,

$$W \ll f_{coh} \quad (9.29)$$

or equivalently,

$$T_m \ll 1/W \quad (9.30)$$

$$\begin{aligned}
z_I(t) + jz_Q(t) &= \frac{1}{2} (s_I(t) + js_Q(t))(H_I + jH_Q) = \\
&= e_s(t)e^{j\theta_s(t)} \cdot ae^{j\phi} = e_z(t)e^{j\theta_z(t)}
\end{aligned} \tag{9.37}$$

$$\boxed{z(t) = ae_s(t) \cos(\omega_c t + \theta_s(t) + \phi)} \tag{9.38}$$

$$p_a(x) = \frac{2x}{b} e^{-x^2/b}, \quad x \geq 0 \quad (\text{Rayleigh distribution}) \tag{9.39}$$

where,

$$E\{a\} = \frac{1}{2} \sqrt{\pi b} \tag{9.40}$$

$$E\{a^2\} = b \tag{9.41}$$

and,

$$p_\phi(y) = \begin{cases} 1/2\pi & , \quad -\pi \leq y \leq \pi \\ 0 & , \quad \text{otherwise} \end{cases} \tag{9.42}$$

If we assume uncoded equally likely binary signals over a Rayleigh fading channel ($z_1(t) = as_1(t), z_0(t) = as_0(t)$), then the bit error probability of the ideal coherent ML receiver is ($0 < d^2 = \frac{D_{s_1, s_0}^2}{2E_{b, sent}} \leq 2$)

$$P_b = \int_0^\infty \Pr\{\text{error}|a\} p_a(x) dx = E\{\Pr\{\text{error}|a\}\} \quad (9.43)$$

$$\begin{aligned} P_b &= \int_0^\infty Q(\sqrt{d^2 x^2 E_{b, sent} / N_0}) \frac{2x}{b} e^{-x^2/b} dx = \\ &= -e^{-x^2/b} Q(x\sqrt{d^2 E_{b, sent} / N_0}) \Big|_0^\infty - \int_0^\infty (-e^{-x^2/b}) \\ &\quad \left(\frac{-\sqrt{d^2 E_{b, sent} / N_0}}{\sqrt{2\pi}} e^{-\frac{x^2 d^2 E_{b, sent} / N_0}{2}} \right) dx = \\ &= \frac{1}{2} - \sqrt{d^2 E_{b, sent} / N_0} \cdot \beta \underbrace{\int_0^\infty \frac{e^{-x^2/2\beta^2}}{\beta\sqrt{2\pi}} dx}_{1/2} \end{aligned} \quad (9.44)$$

$$\mathcal{E}_b = E\{a^2\}E_{b,sent} = bE_{b,sent} \quad (9.45)$$

$$P_b = \frac{1}{2} \left(1 - \sqrt{\frac{d^2 \mathcal{E}_b / N_0}{2 + d^2 \mathcal{E}_b / N_0}} \right) = \frac{1}{2 + d^2 \mathcal{E}_b / N_0 + \sqrt{2 + d^2 \mathcal{E}_b / N_0} \sqrt{d^2 \mathcal{E}_b / N_0}}$$

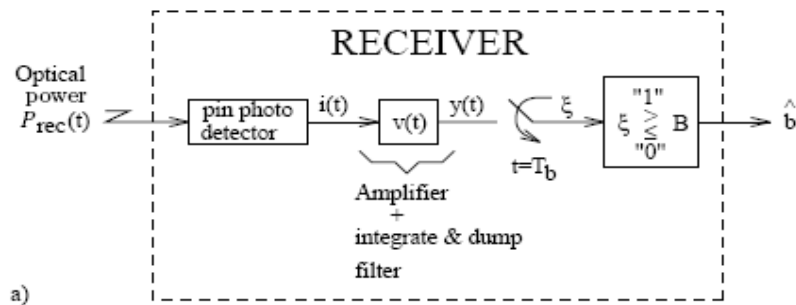
\mathcal{E}_b / N_0 “large”
 \downarrow
 $\approx \frac{1}{2d^2 \mathcal{E}_b / N_0}$
(9.46)

where $d^2 = 2$ for antipodal signals and $d^2 = 1$ for orthogonal signals.

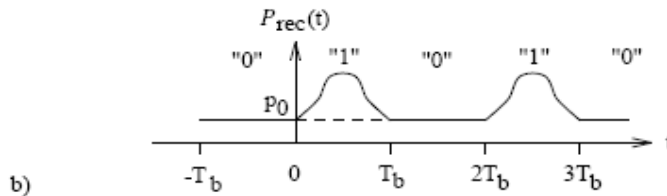
Observe the dramatic increase in P_b due to the Rayleigh fading channel. P_b is no longer exponentially decaying in \mathcal{E}_b / N_0 , it now decays essentially as $(\mathcal{E}_b / N_0)^{-1}$!

DIVERSITY IS NEEDED!

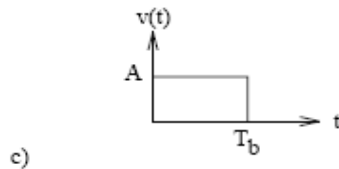
Fig. 7.8:



"0": p_0
 "1": $p_0 + p(t)$



Received optical power.



$$P_{rec}(t) = p_0 + \sum_{i=-\infty}^{\infty} m[i]p(t - iT_b), \quad m[i] \in \{0, 1\}, \quad -\infty \leq t \leq \infty \quad (7.31)$$

$$\begin{aligned} \xi &= y(T_b) = \int_{-\infty}^{\infty} i(\tau)v(T_b - \tau)d\tau = A \int_0^{T_b} i(\tau)d\tau = \\ &= A \int_0^{T_b} (i_r(t) + i_d(t))dt = AqN_{T_b} \end{aligned} \quad (7.32)$$

q=charge of an electron.
 id(t)="dark current".

Bit error probability:

$$\begin{aligned} P_b &= P_0 \underbrace{Prob\{\text{error}|m_0 \text{ sent}\}}_{P_F} + P_1 \underbrace{Prob\{\text{error}|m_1 \text{ sent}\}}_{P_M} \\ &= P_0 Prob\{\xi > B|m_0 \text{ sent}\} + P_1 Prob\{\xi \leq B|m_1 \text{ sent}\} = \\ &= P_0 Prob\{\mathcal{N}_{T_b} > (B/Aq)|m_0 \text{ sent}\} + \\ &\quad + P_1 Prob\{\mathcal{N}_{T_b} \leq (B/Aq)|m_1 \text{ sent}\} \end{aligned} \quad (7.33)$$

$$\begin{aligned} P_F &= Prob\{\mathcal{N}_{T_b} > \alpha|m_0 \text{ sent}\} = \sum_{n=\alpha+1}^{\infty} \frac{\mu_0^n e^{-\mu_0}}{n!} \\ P_M &= Prob\{\mathcal{N}_{T_b} \leq \alpha|m_1 \text{ sent}\} = \sum_{n=0}^{\alpha} \frac{\mu_1^n e^{-\mu_1}}{n!} \\ \alpha &= B/Aq \end{aligned} \quad (7.35)$$

Exact expressions!

We need the averages!

$$\begin{aligned}
 P_b &\approx Q(\varrho) \\
 \varrho &= \sqrt{\mu_1} - \sqrt{\mu_0}
 \end{aligned}
 \tag{7.39}$$

$$\begin{aligned}
 \mu_0 &= E\{\mathcal{N}_{T_b} | m_0 \text{ sent}\} = \int_0^{T_b} \left(\frac{\eta}{hf} p_0 + \mathcal{I}_d \right) dt = \mathcal{I}_d T_b + \frac{\eta\lambda}{hc} p_0 T_b \\
 \mu_1 &= E\{\mathcal{N}_{T_b} | m_1 \text{ sent}\} = \mu_0 + \frac{\eta\lambda}{hc} \int_0^{T_b} p(t) dt = \mu_0 + \frac{\eta\lambda}{hc} \cdot \mathcal{E}_p
 \end{aligned}
 \tag{7.34}$$

$$\mathcal{I}_d = i_d/q$$

$$P_b \approx Q(\varrho)$$

$$\varrho = \sqrt{\mu_1 + \sigma_w^2} - \sqrt{\mu_0 + \sigma_w^2} = \frac{\mu_1 - \mu_0}{\sqrt{\mu_0 + \sigma_w^2} + \sqrt{\mu_1 + \sigma_w^2}}$$

(7.46)

$$\varrho = \frac{\frac{\eta\lambda}{hc} \mathcal{P}_p T_b}{\sqrt{\mathcal{I}_d T_b + \frac{\eta\lambda}{hc} p_0 T_b + k_\sigma T_b} + \sqrt{\mathcal{I}_d T_b + \frac{\eta\lambda}{hc} (p_0 T_b + \mathcal{P}_p T_b) + k_\sigma T_b}} \quad (7.47)$$

$$\mathcal{P}_p = \mathcal{E}_p / T_b$$

$$\frac{\mathcal{P}_{p,1}}{\sqrt{R_{b,1}}} = \frac{\mathcal{P}_{p,2}}{\sqrt{R_{b,2}}} \quad (7.48)$$